

**DOES IMPROVING EARLY PARENTING PRACTICES OPTIMIZE  
WHITE MATTER AND GLOBAL STRUCTURAL NETWORK  
MATURATION? A RANDOMIZED CONTROLLED TRIAL**

by

Hung-Wei Bernie Chen

A dissertation submitted to the Faculty of the University of Delaware in partial fulfillment of the requirements for the degree of Doctor of Philosophy in Psychological and Brain Sciences, Clinical Science Concentration

Summer 2025

© 2025 Hung-Wei Bernie Chen  
All Rights Reserved

**DOES IMPROVING EARLY PARENTING PRACTICES OPTIMIZE  
WHITE MATTER AND GLOBAL STRUCTURAL NETWORK  
MATURATION? A RANDOMIZED CONTROLLED TRIAL**

by

Hung-Wei Bernie Chen

Approved: \_\_\_\_\_  
Robert West, Ph.D.  
Chair of the Department of Psychological and Brain Sciences

Approved: \_\_\_\_\_  
Caleb Everett, Ph.D.  
Dean of the College of Arts & Sciences

Approved: \_\_\_\_\_  
Louis F. Rossi, Ph.D.  
Vice Provost for Graduate and Professional Education and  
Dean of the Graduate College

I certify that I have read this dissertation and that in my opinion it meets the academic and professional standard required by the University as a dissertation for the degree of Doctor of Philosophy.

Signed:

---

Mary Dozier, Ph.D.  
Professor in charge of dissertation

I certify that I have read this dissertation and that in my opinion it meets the academic and professional standard required by the University as a dissertation for the degree of Doctor of Philosophy.

Signed:

---

Jean-Philippe Laurenceau, Ph.D.  
Member of dissertation committee

I certify that I have read this dissertation and that in my opinion it meets the academic and professional standard required by the University as a dissertation for the degree of Doctor of Philosophy.

Signed:

---

Timothy Vickery, Ph.D.  
Member of dissertation committee

I certify that I have read this dissertation and that in my opinion it meets the academic and professional standard required by the University as a dissertation for the degree of Doctor of Philosophy.

Signed:

---

Nim Tottenham, Ph.D.  
Member of dissertation committee

I certify that I have read this dissertation and that in my opinion it meets the academic and professional standard required by the University as a dissertation for the degree of Doctor of Philosophy.

Signed:

---

Emilio Valadez, Ph.D.  
Member of dissertation committee

## ACKNOWLEDGMENTS

This research was supported by the National Institute of Mental Health (R01MH074374) awarded to Mary Dozier, Ph.D. I am deeply grateful to the families who have continuously participated in this study for the past decade. This work would not have been possible without their involvement.

I extend my heartfelt appreciation to my Ph.D. advisor, Mary Dozier, Ph.D., whose profound wisdom, unwavering support, and mentorship have shaped my identity as a scientist and clinician. I also thank my dissertation committee, Nim Tottenham, Ph.D., Emilio Valadez, Ph.D., Jean-Philippe Laurenceau, Ph.D., and Timothy Vickery, Ph.D., for their thoughtful guidance and feedback throughout this process.

I am sincerely thankful to the members of the Attachment and Biobehavioral Catch-up (ABC) research team for their collaboration and encouragement. Lastly, I dedicate this work to my chosen and biological families, whose love and support have sustained me through every step of this journey.

## TABLE OF CONTENTS

LIST OF TABLES .....	viii
LIST OF FIGURES .....	ix
ABSTRACT .....	xi

### Chapter

1	INTRODUCTION.....	1
1.1	Synopsis of Human Brain Development .....	2
1.2	White Matter Maturation.....	3
1.3	Early Parenting Environment .....	7
1.4	The Sequelae of Childhood Maltreatment on Structural Brain Development .....	8
1.5	The Sequelae of Childhood Maltreatment on Brain Connectivity .....	10
1.6	The Sequelae of Childhood Maltreatment on Network Architecture.....	11
1.7	Early Parenting Intervention.....	13
1.8	The Current Study .....	14
1.9	Hypotheses .....	15
2	METHODS.....	16
2.1	Participants .....	16
2.2	Procedure.....	22
2.3	Neuroimaging .....	22
2.4	Preprocessing.....	23
2.5	Estimation of Fractional Anisotropy (FA) and Mean Diffusivity (MD). 24	
2.6	Estimation of Global Network Characteristics .....	26
2.7	Analytic Strategy .....	27
3	RESULTS.....	29
3.1	White Matter Structures .....	29
3.1.1	Model Development .....	29
3.1.2	Association Fiber.....	30
3.1.3	Commissural Fiber .....	34

3.1.4	Projection Fiber .....	37
3.1.5	Summary of Three Major White Matter Structures with FA .....	40
3.2	Global Network Characteristics .....	41
3.2.1	Model Development .....	41
3.2.2	Density.....	42
3.2.3	Global Efficiency.....	43
3.2.4	Small Worldness.....	45
3.3	Post-Hoc Analyses on White Matter Structures with Mean Diffusivity .	47
3.3.1	Association Fiber .....	47
3.3.2	Commissural Fiber .....	49
3.3.3	Projection Fiber .....	51
3.3.4	Summary of Post-Hoc Analyses on Three Major White Matter Structures with MD .....	53
3.4	Exploratory Analysis of Individual White Matter Fasciculi .....	54
4	DISCUSSION.....	59
4.1	Group Differences in the Developmental Trajectory of White Matter Fiber Structures .....	60
4.2	Maltreatment-Specific Differences in the Developmental Trajectory of Global Network Characteristics .....	63
4.3	Group Differences in Neuroplasticity .....	64
4.4	Exploratory Analyses on Individual White Matter Fasciculi .....	69
4.5	Strengths and Limitations .....	71
4.6	Conclusion.....	73
	REFERENCES .....	74
Appendix		
A	IRB/HUMAN SUBJECTS APPROVAL.....	86

## LIST OF TABLES

Table 1. Demographic Data.....	19
Table 2. White Matter Atlases.....	25
Table 3. Fixed Effects for Association Fiber.....	31
Table 4. Fixed Effect Estimates Including Random Slope for Association Fibers .....	33
Table 5. Fixed Effects for Commissural Fiber .....	34
Table 6. Fixed Effect Estimates Including Random Slope for Commissural Fibers....	36
Table 7. Fixed Effects for Projection Fiber .....	37
Table 8. Fixed Effect Estimates Including Random Slope for Projection Fibers .....	39
Table 9. FDR Correction for Quadratic Age by Group Effects .....	40
Table 10. Fixed Effects for Density .....	42
Table 11. Fixed Effects for Global Efficiency .....	44
Table 12. Fixed Effects for Small Worldness .....	46
Table 13. Fixed Effects for Association Fiber.....	48
Table 14. Fixed Effects for Commissural Fiber .....	50
Table 15. Fixed Effects for Projection Fiber .....	52
Table 16. Exploratory Analysis of Individual White Matter Fasciculi .....	55

## LIST OF FIGURES

Figure 1.	Illustrations of FA Values in Different Neural Processes .....	5
Figure 2.	Illustrations of MD Values in Different Neural Processes .....	6
Figure 3.	Association Fiber FA Trajectories by Intervention Groups. Spaghetti plot shows individual trajectories (thin grey lines) of FA across time (in years). Thick solid lines represent group-level fitted regression lines. ABC, DEF, and Low-Risk groups are shown in green, orange, and purple, respectively. ....	32
Figure 4.	Commissural Fiber FA Trajectories by Intervention Groups. Spaghetti plot shows individual trajectories (thin grey lines) of FA across time (in years). Thick solid lines represent group-level fitted regression lines. ABC, DEF, and Low-Risk groups are shown in green, orange, and purple, respectively. ....	35
Figure 5.	Projection Fiber FA Trajectories by Intervention Groups. Spaghetti plot shows individual trajectories (thin grey lines) of FA across time (in years). Thick solid lines represent group-level fitted regression lines. ABC, DEF, and Low-Risk groups are shown in green, orange, and purple, respectively. ....	38
Figure 6.	Density Trajectories by Intervention Groups. Spaghetti plot shows individual trajectories (thin grey lines) of density across time (in years). Thick solid lines represent group-level fitted regression lines. ABC, DEF, and Low-Risk groups are shown in green, orange, and purple, respectively. ....	43
Figure 7.	Global Efficiency Trajectories by Intervention Groups. Spaghetti plot shows individual trajectories (thin grey lines) of global efficiency across time (in years). Thick solid lines represent group-level fitted regression lines. ABC, DEF, and Low-Risk groups are shown in green, orange, and purple, respectively. ....	45

Figure 8.	Small Worldness Trajectories by Intervention Groups. Spaghetti plot shows individual trajectories (thin grey lines) of small worldness across time (in years). Thick solid lines represent group-level fitted regression lines. ABC, DEF, and Low-Risk groups are shown in green, orange, and purple, respectively. ....	47
Figure 9.	Association Fiber MD Trajectories by Intervention Groups. Spaghetti plot shows individual trajectories (thin grey lines) of MD across time (in years). Thick solid lines represent group-level fitted regression lines. ABC, DEF, and Low-Risk groups are shown in green, orange, and purple, respectively. ....	49
Figure 10.	Commissural Fiber MD Trajectories by Intervention Groups. Spaghetti plot shows individual trajectories (thin grey lines) of MD across time (in years). Thick solid lines represent group-level fitted regression lines. ABC, DEF, and Low-Risk groups are shown in green, orange, and purple, respectively. ....	51
Figure 11.	Projection Fiber MD Trajectories by Intervention Groups. Spaghetti plot shows individual trajectories (thin grey lines) of MD across time (in years). Thick solid lines represent group-level fitted regression lines. ABC, DEF, and Low-Risk groups are shown in green, orange, and purple, respectively. ....	53
Figure 12.	Predicted FA and MD Trajectories by Group. This figure illustrates the differences in developmental patterns between groups. Solid lines represent FA growth trajectories, and the dotted lines represent MD growth trajectories. ....	61
Figure 13.	Conceptual Depiction of Associations between SES and White Matter Development (Adapted from Tooley et al., 2021). The black line represents low SES, and the magenta line represents high SES. This figure shows that at the global level, low SES children showed time-limited accelerated maturation of white matter development from middle childhood to adolescence (blue-shaded area). ....	67

## ABSTRACT

A high-quality early parenting environment, involving a sensitive and nurturing caregiver, has a profound, lasting impact on human development. In contrast, exposure to childhood maltreatment jeopardizes brain development and heightens risks for developing psychopathology later in life. If improving the early parenting environment alters the neural developmental trajectory following experiences of childhood maltreatment, then we may be able to mitigate the risks for mental health problems. By leveraging the longitudinal follow-up data of a randomized controlled trial of the Attachment and Biobehavioral Catch-up (ABC) intervention, the present study sought to understand if ABC participation during infancy altered the developmental trajectories of white matter microstructure and global network characteristics, relative to a control intervention. A low-risk sample without prior history of maltreatment was included for reference. The growth trajectories of commissural, projection, and association fibers, as well as graph density, global efficiency, and small worldness were examined. Results indicated that ABC adolescents exhibited a nonlinear trajectory of white matter development, marked by an initial decline followed by later increases in fractional anisotropy (FA), suggesting extended neuroplasticity. Conversely, control and low-risk adolescents exhibited more accelerated maturation, with linear increases in FA and earlier signs of myelination compared to ABC. At the global level, ABC adolescents maintained stable levels of global efficiency and small worldness over time, while control and low-risk youth showed age-related declines. The findings highlight the potential for

early sensitive and nurturing parenting to foster neuroplasticity and support adaptive reorganization.

## **Chapter 1**

### **INTRODUCTION**

Sensitive and nurturing parenting provides the optimal early environment for adaptive brain and psychosocial development (Bick & Nelson, 2016, van der Voort et al., 2014). In contrast, exposure to childhood maltreatment in the form of physically and emotionally unavailable and/or abusive parenting has a profound, lasting, negative impact on the child. The exposure to childhood maltreatment not only alters the functions, structures, and the overall network architecture of the child's brain (Callaghan & Tottenham, 2016; Gee et al., 2013; Puetz et al., 2016; Steenhoff et al., 2019; Teicher et al., 2016), but also promotes the development of psychopathology (Drury et al., 2016; Jaffee, 2017). Early parenting interventions that increase parental responsiveness and sensitivity to child distress have shown positive outcomes on the child's development (Letarte et al., 2010; Swenson et al., 2010). The Attachment and Biobehavioral Catch-up Intervention (ABC; Dozier & Bernard, 2019) is an example of an early parenting intervention designed to enhance the quality of parenting practices among families that are at risk for child maltreatment. The ABC intervention has been rigorously examined using randomized controlled trials (RCTs) and has shown positive down-stream neurodevelopmental and psychological outcomes for children whose parents received the ABC intervention (Bernard, Dozier, et al., 2015; Bernard, Hostinar, et al., 2015; Bick et al., 2018; Garnett et al., 2020; Tabachnick et al., 2019; Valadez et al., 2020; Valadez et al., 2024). Given that adolescence is a sensitive period for white matter development (Kolb & Gibb, 2011; Miller et al., 2012; Schumacher et

al., 2021), divergent neurodevelopmental trajectories may emerge during this time in both typically developing adolescents and those who experienced childhood maltreatment. Because ABC RCTs have shown positive causal neurodevelopmental outcomes for those who received the intervention, participation in ABC during infancy could change the trajectory of white matter development in adolescence. Therefore, using multi-timepoint diffusion magnetic resonance imaging (dMRI) data, the present study sought to understand whether ABC participation causally alters the developmental trajectories of white matter microstructure and global network characteristics, relative to adolescents in a control intervention, as well as in a group of adolescents who were at low risk for childhood maltreatment.

### **1.1 Synopsis of Human Brain Development**

The human brain follows a protracted, nonlinear course of neurodevelopment (Nelson et al., 2019; Tottenham, 2020), reaching its peak of maturation around the third decade of life (Berens & Nelson; 2019; Bick & Nelson, 2016). The brain also develops in a hierarchical manner, with earlier-developing neural architecture posing a cascade-like, down-stream influence on the development of subsequent cortices and circuits (Berens & Nelson; 2019; Bick & Nelson, 2016; Tau & Peterson, 2010; Tottenham, 2020). The cortical and subcortical maturation begins at the most biologically basic systems that support critical life, motor, and sensory functioning (e.g., brainstem, motor cortex, visual cortices; Bick & Nelson, 2016; Kolb & Gibb, 2011), and continues through more complex systems that support the regulation of higher-order processes (e.g., prefrontal cortex, PFC; Berens & Nelson; 2019). Observationally, humans' behavioral developmental milestones (Sheldrick et al., 2019), from somatosensory capacity supporting object manipulation and space

navigation to complex behaviors that require higher-order cognitive and executive functioning, closely mirror this sequence of brain development.

## 1.2 White Matter Maturation

*White matter* refers to the neural tissue filled with nerve fibers, such as axons (Moini & Piran, 2020). The term “white matter” gets its name from its white, glossy appearance caused by lipid-rich cellular membranes, resulting from a neurodevelopmental process called *myelination*. Myelination is performed by *oligodendrocytes* and increases the speed of intra-neuron communications (Gao et al., 2009; Tau & Peterson, 2010). Oligodendrocytes are a type of neuroglia in the central nervous system (Moini & Piran, 2020). Their main function is producing myelin, an insulating layer made of lipid-rich cellular membrane that wraps around the axolemma (the membrane enclosing an axon) to aid in the transmission and acceleration of neural signals between neurons (Moini & Piran, 2020). Myelination follows a protracted developmental course that begins to accelerate during adolescence and continues with a curvilinear growth pattern (Bethlehem et al., 2022; Kolb & Gibb, 2011; Miller et al., 2012). As with cortical and subcortical maturation, white matter develops in a hierarchical fashion (Lebel et al., 2012; Tamnes et al., 2018), starting with neural fibers connecting the two hemispheres (i.e., commissural fibers, and fibers connecting the cerebral cortex with lower brain regions and the spinal cord (i.e., projection fibers; Lebel et al., 2012). The neural fibers connecting the cortical areas ipsilaterally (i.e., association fibers) mature later. The fibers connecting the frontal and temporal cortices develop the slowest.

*In vivo* myelination processes are typically measured through diffusion-weighted imaging (DWI; Rowe et al., 2016). DWI is an application of magnetic

resonance imaging (MRI) that manipulates magnetic gradients (along the  $x$ ,  $y$ , and  $z$  axes) to measure the magnitude of hydrogen proton signals along one axis (Rowe et al., 2016). Aggregating all information from all three dimensions can provide insights into the direction of the signals. A water molecule consists of two hydrogen atoms and one oxygen atom. Water is found in all body tissues, including the brain. Therefore, DWI data enable us to understand how water molecules diffuse across different brain tissues. Diffusion tensor imaging (DTI) is a mathematical modeling method that fits DWI data using eigenvalues ( $\lambda$ ) and eigenvectors, which describe the shape and orientation of diffusion within a voxel. Fractional anisotropy (FA), derived from the DTI approach, is one of several ways to summarize the strength of water diffusion in a given space and is calculated using eigenvalues:

$$\text{Fractional Anisotropy (FA)} = \sqrt{\frac{3}{2} \left( \frac{(\lambda_1 - \hat{\lambda})^2 + (\lambda_2 - \hat{\lambda})^2 + (\lambda_3 - \hat{\lambda})^2}{\lambda_1^2 + \lambda_2^2 + \lambda_3^2} \right)}$$

*Note:  $\lambda_1$ ,  $\lambda_2$ , and  $\lambda_3$  represent the eigenvalues in a three-dimensional space, and  $\hat{\lambda}$  represents their mean.*

FA may vary from 0 to 1, respectively termed as isotropy and anisotropy. As FA increases, there is an increasing magnitude of diffusion along one direction. High FA values typically indicate highly directional diffusion, such as along the axis of densely packed, coherently aligned, and myelinated axons (Rowe et al., 2016). See Figure 1.

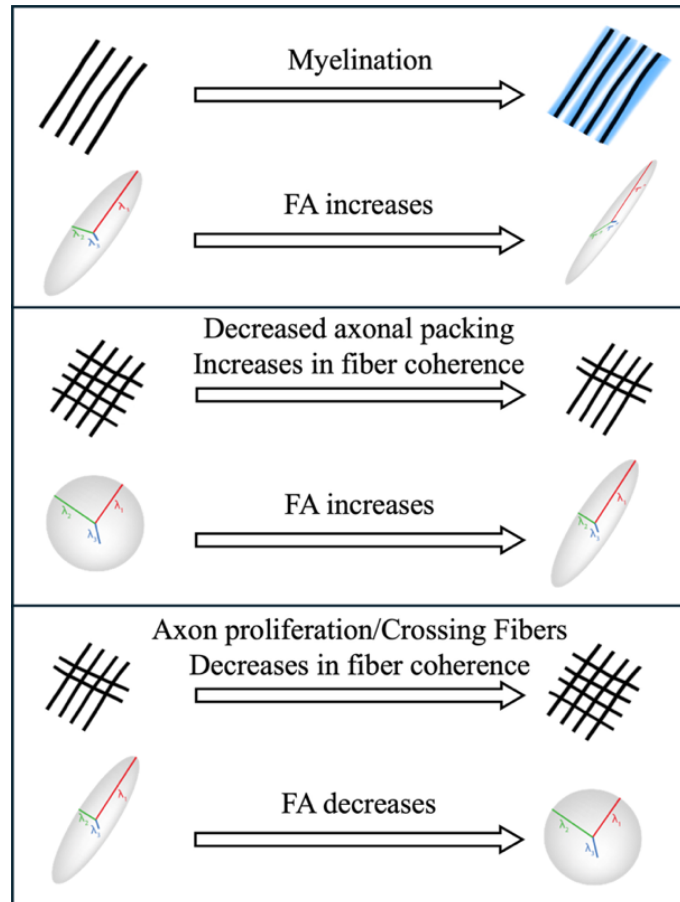


Figure 1. Illustrations of FA Values in Different Neural Processes

In the tissue, high FA values may indicate that the lipid-rich cellular membrane in the myelin effectively traps water, preventing water molecules from moving freely and causing them to travel mainly along the axon. While high FA generally signifies the maturation of myelination, it can also be affected by other factors such as fiber coherence, crossing fibers, and axon diameter (Figley et al., 2022). Therefore, FA should be interpreted in conjunction with other microstructural metrics, such as mean diffusivity (MD). Mean diffusivity (MD) measures the overall magnitude of water diffusion across all directions. It is computed as:

$$\text{Mean Diffusivity (MD)} = \frac{\lambda_1 + \lambda_2 + \lambda_3}{3}$$

While FA provides information about directional coherence, MD offers insight into the overall permeability or compactness of the tissue. For example, increased MD may reflect greater extracellular space or less restricted diffusion, whereas decreased MD suggests more densely packed tissue. See Figure 2.

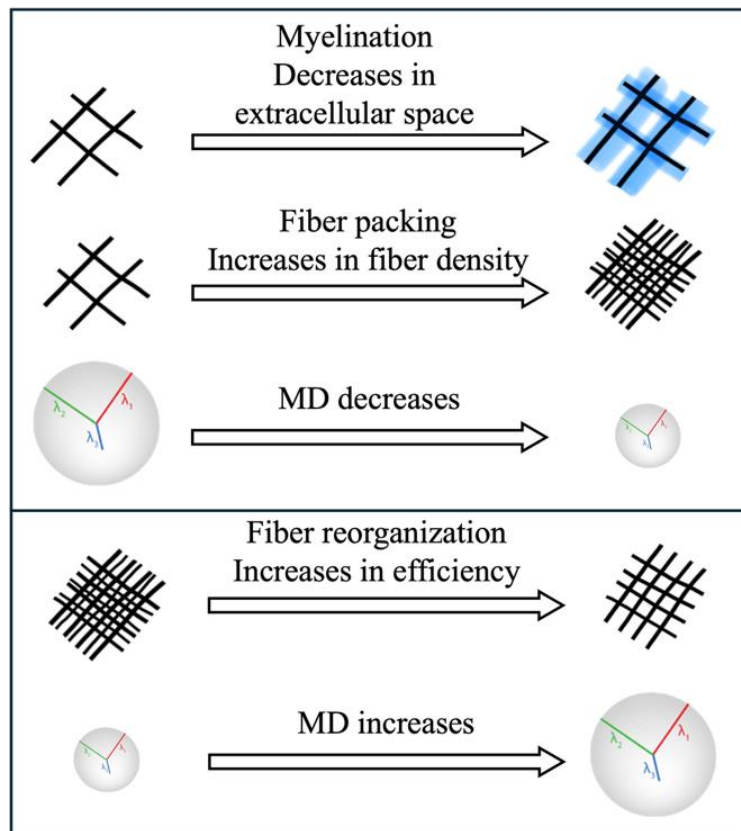


Figure 2. Illustrations of MD Values in Different Neural Processes

Together, FA and MD can help differentiate whether observed diffusion changes stem from increased fiber organization or alterations in tissue density, thereby aiding in the interpretation of white matter development (Figley et al., 2022).

### **1.3 Early Parenting Environment**

The quality of the early parenting environment has a tremendous impact on human development. During the early years of life, the infant's brain requires positive environmental inputs and stimulation (Berens & Nelson; 2019; Bick & Nelson, 2016). Positive parental inputs are essential to create an enriched environment. To a developing infant, a sensitive caregiver is someone who encourages exploration, embraces expressions of emotional vulnerability, and provides a physical and emotional shelter away from threats and dangers (Berens & Nelson; 2019; Tronick, 2007; van der Voort et al., 2014). According to attachment theory (Ainsworth, 1974; Bowlby, 1977), human species, like other altricial and semi-altricial animals, are programmed to rely on a caregiver to maintain life, protect from threats, and soothe during moments of distress. Human infants do so by forming an attachment relationship with the primary caregiver (Ainsworth, 1974). Therefore, attachment is thought to reflect an evolutionally adaptive, survival strategy (Ainsworth, 1974; Bowlby, 1977; Hofer, 2006). The innate proximity-seeking behavior towards a trusted caregiver has been imperative for maximizing survival from an evolutionary standpoint. A trusted, available, nurturing, and sensitive caregiver can serve as a secure base. Infants utilize the secure base to explore surrounding environments to increase opportunities for learning. During moments of distress, infants who form a secure attachment with their caregiver retreat to their caregiver. In this encounter, the caregiver actively soothes the infant and serves as a co-regulator of emotions (Hofer,

2006). Over time, the child takes over the regulatory responsibility themselves. Inside the infant's brain, these emotion regulation experiences scaffolded by their parents shape the communication patterns between neurons and circuits that are important for emotion regulation, one of the complex systems of higher-order processes (Fox & Rutter, 2010; Tottenham, 2012). However, when parents provide problematic inputs (e.g., abuse or neglect), the communications between neurons and more complex circuits are disrupted (Callaghan & Tottenham, 2016; Steenhoff et al., 2019). Given that human infants are evolutionally expected to have a caregiver who tends to their needs and nurtures during moments of distress, an abusive or neglecting caregiver not only disrupts this expectation but also introduces significant challenges to infants' brain development (Tottenham, 2013).

#### **1.4 The Sequelae of Childhood Maltreatment on Structural Brain Development**

Childhood maltreatment is associated with alterations in global brain morphology, including changes in the cortical and subcortical structures (Callaghan & Tottenham, 2016; Tozzi et al., 2020). The impact of child maltreatment has also been extensively documented at several PFC sub-regions implicated in more complex emotional and cognitive processes (Bick & Nelson, 2016). For example, the PFC and the complex emotional and cognitive processes develop in tandem and are highly sensitive to stress (Bick & Nelson, 2016; Fuster, 2001). Among individuals exposed to child maltreatment, reductions in several sub-regions of the PFC have been observed, including the orbitofrontal cortex (OFC, associated with reinforcement-based decision making and emotion regulation; Ochsner and Gross, 2005), the superior frontal gyrus (associated with working memory; Kelly et al., 2013), and dorsal lateral PFC (associated with emotional and executive control; Edmiston et al., 2011). In addition,

some of the research focus has been placed on the limbic circuitry, particularly the amygdala and hippocampus, due to its role in emotion regulation, stress reactivity, and learning and memory (Phelps, 2004). Cross-sectional studies have reported volumetric reductions in the amygdala and hippocampus for children who experienced childhood maltreatment, compared to those who did not (De Brio et al., 2013; McCrory et al., 2011).

In recent years, there has been a growing interest in understanding the sequelae of child maltreatment on the development of white matter microstructure. Several DTI studies reported a reduction of FA in the commissural fibers (corpus callosum and fornix) and association fibers (cingulum, inferior fronto-occipital fasciculus, superior longitudinal fasciculus, and uncinate fasciculus; Govindan et al., 2010; Huang et al., 2012; Jackowski et al., 2008; McCarthy-Jones et al., 2018) when comparing individuals who experienced child maltreatment with those who did not. These impacted white matter tracts connect cortical regions that are important for higher-level cognitive and emotional functioning (Bick & Nelson, 2016). Furthermore, in recent years, a few longitudinal dMRI studies (Lebel et al., 2012; Tamnes et al., 2018) have examined the growth trajectories of major white matter tracts in a normative sample and characterized adolescence as a sensitive window for myelination processes. However, longitudinal dMRI studies with a sample of previously maltreated youths are extremely rare. To our knowledge, no studies have extensively documented the growth trajectories of white matter tracts following exposure to parenting-related adversity.

While a few correlational studies have demonstrated a potential link between parenting quality and white matter maturation, empirical evidence in this area is

extremely limited. One study (Serra et al., 2016) showed that among adults who self-reported their attachment security with their primary caregiver, higher security correlated with greater FA in the association fibers, including the cingulum, uncinate fasciculus, superior longitudinal fasciculus, and inferior fronto-occipital fasciculus, all of which are important for higher-order emotion-cognition processes. Very little is known about the associations between parenting behaviors and white matter maturation, especially during the sensitive window of myelination in adolescence. Studies have shown that warm and supportive maternal behaviors are associated with grey matter maturation during adolescence (Whittle et al., 2014; Whittle et al., 2016), although the outcomes are not directly related to white matter maturation. While these studies on grey matter maturation are peripheral to white matter maturation, they demonstrated a putative association between quality of parenting and neural anatomical development broadly. Longitudinal empirical evidence from an RCT remains imperative to establish a causal link between quality of parenting and the development of myelination processes. Filling these gaps will be especially valuable for addressing the negative impact of child maltreatment through intervention and preventative programming.

### **1.5 The Sequelae of Childhood Maltreatment on Brain Connectivity**

Connectivity-based analyses have emerged as a vital tool to understand how information between neurons and circuits is exchanged. Findings from connectivity-based studies provide important insights into the way in which experiences of child maltreatment disrupt neural communications, and consequently confer risks for poor outcomes. Childhood maltreatment is associated with altered frontal-limbic functional connectivity (Gee et al., 2013; Teicher et al., 2016). In addition, among adults who

retrospectively recalled experiences of childhood maltreatment, the maltreated group relative to the comparison group demonstrated increased amygdala-PFC connectivity during an emotional reactivity task, suggesting a cognitive inefficiency of top-down processes recruitment even years after exposure to child maltreatment (Jedd et al., 2015). A recent study demonstrated decreased structural connectivity in the accumbens white matter tracts, implicated in reward processing and learning, among adolescents who endorsed experiences of childhood maltreatment (Kennedy et al., 2021). The findings delineating the communication patterns between cortices help us understand how the experiences of child maltreatment impact the neural circuits.

## **1.6 The Sequelae of Childhood Maltreatment on Network Architecture**

During the past decade emerging studies have focused on the impact of childhood maltreatment on the developing *connectome*. Simply put, the connectome is the mapping of functional or structural brain connections. The study of connectome is called *connectomics* (Bullmore & Sporns, 2009). A growing number of dMRI studies (Ohashi et al., 2017; Puetz et al., 2016; Teicher et al., 2016) have shifted analytic strategies from seed-based (one region to another) connectivity to examining the brain as a complex, dynamic network.

When applying the mathematical principles of *graph theory* to connectome, we can begin to describe the ways in which systems of the brain communicate with each other (Bullmore & Sporns, 2009; Kim & Min, 2020). A network consists of nodes and edges. In the context of a structural brain network, brain regions and the neural fibers connecting the regions can be thought of as nodes and edges, respectively. There are several ways to quantify network characteristics. To name a few, *graph density* represents the ratio between the numbers of available and all the possible edges in the

network, which can be seen as the degree of connectedness. *Global efficiency* represents the shortest distance (by the numbers of edges) across a network, with higher efficiency indicating easier or lesser degree of effort that is required for communications. A cluster of connected nodes can form a small community. *Clustering coefficient* is the likelihood that a node is connected to a neighboring community. If the clustering coefficient is high, it indicates that any given node in the network is highly probable to also be part of a closely connected community. *Characteristic path length* represents the average distance of each edge. Lower characteristic path length may indicate that all nodes are more closely connected with each other. *Small worldness* combines high clustering and low characteristic path length, reflecting an optimal balance between segregation and integration. High small worldness indicates the brain network is both locally clustered and globally efficient. In this case, the brain regions form tightly connected groups while still maintaining short paths to other regions, allowing for fast and coordinated communication. This balance between segregation and integration supports flexible and efficient information processing. Briefly summarized, a healthy connectome is often characterized by high graph density, high global efficiency, high clustering coefficient, low characteristic path length, and high small worldness.

One study examined the impact of childhood maltreatment on structural connectome and found that adults with histories of childhood maltreatment had lower graph density, lower global efficiency, and higher small worldness than those who did not endorse experiences of childhood maltreatment (Ohashi et al., 2017). Puetz et al. (2016) similarly reported lower graph density for pre-teens ( $M_{age} = 10.6$ ,  $SD_{age} = 1.75$  years) who had experienced child maltreatment relative to those who had not. These

results offer powerful insights for understanding the neurodevelopmental sequelae of child maltreatment. Given that adolescence is characterized as a sensitive window for myelination, divergent patterns of myelination processes may emerge among adolescents who experienced childhood maltreatment and non-maltreated counterparts. Yet, longitudinal empirical evidence is extremely scarce. The lack of evidence base for the developmental trajectory of connectome following childhood maltreatment presents a pressing need for empirical investigation.

### **1.7 Early Parenting Intervention**

Given that the quality of parenting practices early in life has a cascade-like influence on child's later psychological and neurobiological development, RCTs have demonstrated that early parenting interventions, designed to improve parenting quality, have causal, positive impacts on children's development (e.g., Bernard, Dozier, et al., 2015; Letarte et al., 2010; Swenson et al., 2010). The ABC intervention (Dozier & Bernard, 2019) is an example of an early intervention focusing on improving the quality of parenting among families at risk for childhood maltreatment. The ABC intervention has three parenting targets: increasing nurturing responsiveness to child distress, increasing parental sensitivity to child non-distress signals, and decreasing frightening and harsh behaviors (Dozier & Bernard, 2019). Parents who were randomly assigned to receive the ABC intervention have shown greater improvement (pre- to post-intervention) in parenting quality when compared to parents who received a control intervention, in terms of greater increases in sensitivity to child's signals, greater increases in showing positive affect towards the child during interactions, and greater decreases in parental intrusiveness (e.g., Bick & Dozier, 2013; Yager et al., 2020). Among families at risk for childhood maltreatment, children

whose parents were randomly assigned to receive the intervention have also shown better neurobiological and psychological outcomes compared to children whose parents received a control intervention. For example, the positive effects have been observed in the development of amygdala-PFC circuitry (Valadez et al., 2024), neural representations of the parent measured with BOLD signals (Valadez et al., 2020), neural activity measured with EEG (Bick et al., 2019), diurnal cortisol regulation (Bernard, Dozier, et al., 2015; Bernard, Hostinar, et al., 2015; Garnett et al., 2020), autonomic nervous system regulation (Tabachnick et al., 2019), DNA methylation (Hoye et al., 2020), parent-child attachment (Bernard et al., 2012), emotion regulation (Lind et al., 2014), executive functioning and inhibitory control (Korom et al., 2021; Lind et al., 2020), and language development (Bernard et al., 2017, Raby et al., 2019). The empirical evidence base for the ABC intervention suggests that improving parenting practices can have causal, profound, lasting benefits for the children's development across multiple levels of analysis. By leveraging a longitudinal follow-up study of an RCT on the ABC intervention, we are well-equipped to examine the causal link between improvement in parenting practices and myelination processes that are prominent during adolescence.

## **1.8 The Current Study**

The goal of the present study was to examine whether early parenting quality causally affects white matter and global structural network maturation by leveraging the longitudinal, multi-timepoint dMRI data from a follow-up study of an RCT assessing the efficacy of the ABC intervention. The present study examined whether ABC participation, relative to a control intervention, causally predicted more optimal trajectories of maturation in major white matter fibers, including the commissural,

projection, and association fibers (**Aim 1**), as well as global network characteristics, including graph density, global efficiency, and small worldness (**Aim 2**). Adolescents who were at low risk for childhood maltreatment were included in the analyses as a reference for the intervention group comparison.

## **1.9 Hypotheses**

We hypothesized that the average FA across major white matter tracts would follow a non-linear course of developmental trajectory, showing a protracted pattern of development. Adolescents in the ABC and low-risk group would show a developmentally adaptive, curvilinear trajectory, whereas those in the DEF group would show a flat, linear developmental trajectory. Similarly, we hypothesized that at the level of global network, the ABC and low-risk group would demonstrate a more developmentally adaptive pattern of maturation, relative to DEF.

## **Chapter 2**

### **METHODS**

#### **2.1 Participants**

The original study is an ongoing research study funded by the National Institute of Mental Health (R01MH074374), assessing the longitudinal outcomes of an RCT for children whose families received the Attachment and Biobehavioral Catch-up (ABC) intervention when they were infants. ABC is a brief (10-session, 1-hour per week), strength-based, home-visiting parenting intervention, designed to promote sensitive parenting in three main behavioral targets: increasing sensitivity to child signals, increasing nurturance to child distress, and decreasing frightening and harsh behaviors. These intervention targets were identified based on empirical findings (e.g., Bernard et al., 2010). Parent coaches trained in ABC conduct the sessions at the target family's home, therefore decreasing challenges involved in transferring skills learned in an office setting to the home. These coaches utilize a manual to guide the delivery of ABC. The intervention targets are introduced sequentially by sessions, allowing time for practice and discussion of intervention targets. Parent coaches support the parents in identifying children's signals and providing responsive care through in-the-moment commenting and feedback to parents (Caron et al., 2018). In addition to the experimental (ABC) intervention, a control intervention, the Developmental Education for Families (DEF), was included as part of the original RCT. DEF is an adaptation of existing interventions (e.g., Ramey et al., 1984) that have been shown to promote development of children's motor skills, cognition, and language abilities. To

distinguish it from ABC, parental sensitivity-related components were removed from DEF.

When recruiting participants for the RCT, 212 families from the Greater Philadelphia Area were referred from Child Protective Services (CPS) due to reports of risk for abuse or neglect (Garnett et al., 2020), and subsequently enrolled in the study. Families were masked regarding their intervention group assignments. At the pre-intervention assessments, children in the two intervention groups did not differ significantly in age or race (Bernard, Dozier, et al., 2015), and parents did not differ significantly in age, educational attainment, race (Bernard et al., 2012), parental sensitivity, or attachment-related representations (Tabachnick et al., 2019). A total of 183 families completed a 24-month post-intervention research visit. At the adolescent follow-up assessments, a total of 186 families (including the low-risk comparison) enrolled.

At the 13-year scan, 135 adolescents (43 ABC, 46 DEF, 46 low-risk) attempted dMRI scanning; 20 (6 ABC, 9 DEF, 5 low-risk) did not complete due to reported discomfort or getting out of the scanner without providing a reason; 2 (1 ABC, 1 DEF) were not able to fit into the scanner; and 7 (1 ABC, 2 DEF, 4 low-risk) had braces. A total of 106 completed the scan (35 ABC, 34 DEF, 37 low-risk).

At the 14-year scan, 113 adolescents (40 ABC, 38 DEF, 35 low-risk) attempted dMRI scanning; 3 (2 DEF, 1 low-risk) did not complete due to reported discomfort or getting out of the scanner without providing a reason; 1 DEF adolescent was not able to fit into the scanner; and 1 ABC adolescent had braces. A total of 108 completed the scan (39 ABC, 35 DEF, 34 low-risk).

At the 15-year scan, 129 adolescents (45 ABC, 48 DEF, 36 low-risk) attempted dMRI scanning; 2 (1 ABC, 1 low-risk) adolescents did not complete due to reported discomfort or getting out of the scanner without providing a reason; 4 (3 DEF, 1 low-risk) were not able to fit into the scanner; and 1 DEF adolescent had a metal implant. A total of 122 completed the scan (44 ABC, 44 DEF, 34 low-risk).

It is important to note that there was a grace period up to 3 months for the 13- and 14-year scans. For example, a participant qualified for a 13-year scan if they were not older than 14 years and 3 months. For the 15-year scan, the age limit was extended to allow as large a sample as possible. As a result, the current age range for the present neuroimaging dataset, aggregating data across adolescent assessments, was 12.950 – 16.757 years ( $M_{age} = 14.465$  years,  $SD_{age} = .905$ ). After excluding data with significant quality-related issues, the final dataset included 90 dMRI images from the 13-year scan, 101 from the 14-year scan, and 109 from the 15-year scan, which is a total of 300 dMRI images. The final dataset represented 145 participants (48 ABC, 52 DEF, 45 low-risk).

Table 1. Demographic Data

	ABC	DEF	Low-Risk	Difference Tests
Total N	48	52	45	
<u>Gender</u>				
Male	26	28	26	$\chi^2(2) = .180, p = .914.$
Female	22	24	19	
<u>Age in Year</u>				
Mean	14.548	14.474	14.356	
SD	.864	.969	.884	$F(2, 297) = 1.103, p = .333.$
Min	13.012	13.019	12.95	
Max	16.532	16.757	16.439	
<u>Race/Ethnicity</u>				
Black	31	29	17	
White	2	6	8	
Multi-/Bi-racial	4	2	9	$\chi^2(10) = 16.477, p = .087.$
Other	1	2	0	
Did not answer	10	13	11	
<u>Hispanic/Latino</u>				
Yes	7	11	9	
No	33	37	27	$\chi^2(4) = 2.890, p = .421.$
Did not answer	8	4	9	

<u>Parental Education</u>				$\chi^2(12) = 36.988, p < .001$ . Low-risk group had more parents with a 4-year degree and fewer who didn't complete high school than expected by chance.
Did not complete HS	14	12	2	
HS Diploma	15	21	11	
GED	6	8	2	
Some college	12	9	19	
4-year degree	0	1	7	
Postgraduate degree	0	0	3	
Did not answer	1	1	1	
<u>Employment</u>				$\chi^2(2) = 13.021, p = .001$ . Low-risk group had significantly fewer unemployed caregivers than expected.
Employed	29	24	38	
Unemployed	14	17	3	
Did not answer	5	11	4	
<u>Government Aid</u>				$\chi^2(2) = 29.636, p < .001$ . Low-risk parents were more likely to report not receiving aid than expected, whereas DEF parents were more likely to report receiving aid.
Received	29	38	9	
Did not receive	18	13	35	
Did not answer	1	1	1	
<u>Averaged Income across Years</u>				$F(2, 128) = 14.120, p < .001$ . Post-hoc Tukey's HSD test: low-risk > ABC (mean diff. = \$32,448, $p = .001$ ) and low-risk > DEF (mean diff. = \$41,821, $p < .001$ ). ABC vs. DEF (mean diff. = \$9,373, $p = .478$ ).
Mean	\$39,313.83	\$29,940.44	\$71,761.63	
Median	\$33,666.67	\$24,000.00	\$55,000.00	
1st Quartile	\$16,750.00	\$13,525.00	\$33,000.00	
3rd Quartile	\$49,416.67	\$45,000.00	\$94,133.33	
Missing (N)	5	5	4	
<u>No High Income Outliers</u>				

Outliers (1.5 x IQR)	1	0	6
Mean	\$36,916.54	\$29,940.44	\$52,835.05
Median	\$33,333.33	\$24,000.00	\$44,000.00
1st Quartile	\$16,575.00	\$13,525.00	\$32,166.67
3rd Quartile	\$49,166.67	\$45,000.00	\$70,000.00

*Note:* IQR stands for interquartile range. IQR = 3rd Quartile – 1st Quartile.

$F(2, 121) = 8.496, p < .001$ . Post-hoc Tukey's HSD test: low-risk > ABC (mean diff. = \$15,918,  $p = .018$ ) and low-risk > DEF (mean diff. = \$22,894,  $p < .001$ ). ABC vs. DEF (mean diff. = \$6,976,  $p = .394$ ).

## 2.2 Procedure

The University of Delaware Institutional Review Board approved all protocols and procedures used in the study. Participant (adolescent) written and oral assents and parental consents were obtained prior to participation in the study. In the 13-, 14-, and 15-year follow-up assessments, adolescent participants who did not meet the exclusion criteria for MRI contraindications (e.g., metal implants, current pregnancy) were acclimated to the scanner using an MRI replica before the scanning session.

## 2.3 Neuroimaging

The neuroimaging data collection took place at the University of Delaware Center for Biomedical and Brain Imaging. Data were acquired using a 3T Magnetom Prisma scanner with a 64-channel head coil. The scanning parameters were consistent with those used in the Human Connectome Project (van Essen et al., 2012) and the Adolescent Brain Cognitive Development Study (Casey et al., 2018). The T1-weighted structural image, across 13-, 14-, and 15-year assessments, was acquired using the following parameters: TR = 2,400 msec, TE = 2.14 msec, flip angle = 78°, field of view = 256 mm<sup>2</sup>, and voxel dimensions = 1 mm<sup>3</sup> isotropic

Diffusion MRI (dMRI) data were acquired using two slightly different acquisition parameters. For approximately half of the sample, dMRI data were acquired using the following parameters: TR = 3,520 msec, TE = 95.2 msec, flip angle = 78°, refocusing flip angle = 160°, voxel dimensions = 1.5 × 1.5 × 1.5 mm<sup>3</sup>, multiband factor = 4, b-values = 1,500 and 3,000 s/mm<sup>2</sup> and 240 diffusion orientations with 3 non-weighted images (b = 0 s/mm<sup>2</sup>) acquired in the anterior-posterior direction, plus one reverse phase-encoding image (b = 0 s/mm<sup>2</sup>). The remaining half were

acquired using b-values = 1,000, 2,000, and 3,000 s/mm<sup>2</sup> with 6 reverse phase-encoding images (b = 0 s/mm<sup>2</sup>).

As noted, there was a slight difference in the b-value schemes across the two acquisition parameters. However, the distribution of participants across groups (ABC, DEF, low-risk) did not significantly differ by the type of acquisition parameter. Specifically, for Parameter 1: ABC = 45, DEF = 39, low-risk = 40. For Parameter 2: ABC = 59, DEF = 65, low-risk = 52. A chi-square test indicated no significant difference across groups,  $\chi^2(2) = .966, p = .617$ , which minimizes concerns that difference of parameters would confound group-related effects. However, given that the switch of parameters occurred at the middle of the data collection effort, the difference of parameters was strongly correlated with participants' age at scan ( $r = .726, p < .001$ ). Because the difference of parameters serves as a proxy of time, including it as a covariate in the group-level analysis would risk statistically removing age-related variance, which is the focus of this present study on developmental trajectories. Moreover, because the difference of parameters is a binary variable, it cannot meaningfully model the curvilinear patterns of change captured by biological age. For these reasons, we determined to not include the difference of parameter in the group-level analysis.

## **2.4 Preprocessing**

The dMRI data were processed using FSL's TOPUP (Andersson et al., 2003; Smith et al., 2004) to correct for susceptibility-induced distortions and EDDY (Andersson & Sotiropoulos, 2016) to correct for eddy current-induced distortions and participant movements. The data were then processed through FSL's DTIFIT (Smith

et al., 2004) to fit diffusion tensors at each voxel to complete data preprocessing steps. Each preprocessed image passed a rigorous pipeline of quality assurance.

## **2.5 Estimation of Fractional Anisotropy (FA) and Mean Diffusivity (MD)**

To prepare the extraction of fractional anisotropy (FA) values for each participant, the preprocessed data underwent FSL's Tract-Based Spatial Statistics (TBSS; Smith et al., 2006) pipeline to complete nonlinear registration to the FMRIB58\_FA template (MNI152 standard space) at 1 mm<sup>3</sup> isotropic, creating skeletonized FA images. This step ensures alignment of all FA data across participants, enabling the subsequent data extraction process using an MNI152-standard-space compatible atlas (i.e., XTRACT tract atlases; Warrington et al., 2020). Individual XTRACT-based white matter atlases were generated and visually inspected for anatomical accuracy. Please see Table 2 for all white matter tract atlases.

Table 2. White Matter Atlases

Association	Commissural	Projection
Arcuate Fasciculus (L/R)	Anterior Commissure	Acoustic Radiation (L/R)
Cingulum Dorsal (L/R)	Forceps Major	Anterior Thalamic Radiation (L/R)
Cingulum Perigenual (L/R)	Forceps Minor	Superior Thalamic Radiation (L/R)
Cingulum Temporal (L/R)	Fornix (L/R)	Optic Radiation (L/R)
Corticospinal Tract (L/R)		Middle Cerebellar Peduncle
Frontal Aslant Tract (L/R)		
Inferior Fronto-Occipital Fasciculus (L/R)		
Inferior Longitudinal Fasciculus (L/R)		
Middle Longitudinal Fasciculus (L/R)		
Superior Longitudinal Fasciculus 1 (L/R)		
Superior Longitudinal Fasciculus 2 (L/R)		
Superior Longitudinal Fasciculus 3 (L/R)		
Uncinate Fasciculus (L/R)		
Vertical Occipital Fasciculus (L/R)		

*Note:* L indicates left; R indicates right.

Lastly, an FSL's native function for mathematical operations on imaging data ("*fslmaths*") was used for data extraction to obtain FA value for each white matter tract atlas for every skeletonized FA image. Post-hoc analysis was performed on mean diffusivity (MD) to complement the interpretation of FA findings. MD skeletonized maps were generated using TBSS's "*tbss\_non\_FA*" script. MD values were extracted from the same XTRACT tract atlases used to obtain FA values.

## **2.6 Estimation of Global Network Characteristics**

Each preprocessed dMRI image along with its respective b-value and b-vector information, was processed through the DSI Studio (Yeh et al., 2013) to generate a "*sc.gz*" file, a DSI Studio-native dMRI metadata format. Following previously established data processing procedures (e.g., Ciavarro et al., 2022; Lee et al., 2023), the subsequent data were reconstructed in a common stereotaxic space by applying the q-space diffeomorphic reconstruction (QSDR) algorithm on the HCP1021 young adult template. During the QSDR reconstruction process, respective T1- and T2-weighted anatomical scans as well as a T1-weighted brain mask were used to increase anatomical accuracy. Whole-brain fiber tracking was performed by a total of 1,000,000 seeds in the entire brain, using deterministic fiber-tracking algorithm. The tracked fiber tracts with lengths shorter than 60 or longer than 300 mm were discarded. Spatial normalization was conducted to ensure the built-in FreeSurfer Segmentation atlas was registered with each dMRI image. The connectivity matrix was estimated by using the count of the connecting tracts passing through the regions of the FreeSurfer Segmentation atlas, and 0.001 of the sums was set as the threshold. The global network characteristics were calculated for density, global efficiency, and small worldness.

## 2.7 Analytic Strategy

Data were analyzed with a mixed-effects modeling approach in R (R Core Team, 2023), using “*lme4*” (Bates et al., 2015) and “*lmerTest*” (Kuznetsova et al., 2017) packages. Mixed-effects modeling accounts for the dependency of repeated measures by modeling individual observations as nested within subjects. This approach offers flexibility, specifically for modeling continuous time with both linear and nonlinear approaches, and enables estimates of within- and between-participant variations (e.g., random effects).

Intervention was dummy coded with ABC as the reference group. To compare ABC to DEF and ABC to low risk, two contrasts were created: 1) DEF v. ABC (DEF = 1, ABC = 0, low risk = 0) and 2) low risk v. ABC (low risk = 1, ABC = 0, DEF = 0). Time was modeled continuously using biological age (age) to capture linear developmental changes. Age was calculated in days from birth to the scanning date and then converted into years by dividing the days by 365.25. After mean-centering, a quadratic term (age<sup>2</sup>) was computed and included to account for nonlinear trajectories. To test intervention differences in developmental change, four interaction terms were created: 1) age by DEF v. ABC, 2) age by low-risk v. ABC, 3) age<sup>2</sup> by DEF v. ABC, and 4) age<sup>2</sup> by low-risk v. ABC.

Model building followed a theory- and fit-driven approach, which began with a baseline model including a random intercept for participants but no predictors. Every model was estimated using maximum likelihood (ML). Additional random effects (e.g., random slopes for age) were fitted sequentially. The model selection process was informed by theory, likelihood ratio tests, and model parsimony. Given simultaneous multiple hypothesis testing on biologically similar constructs, focal effects were

adjusted for their significance levels using false discovery rate (FDR) correction.

Visualization of results was generated using the “*ggplot2*” package (Wickham, 2016).

## Chapter 3

### RESULTS

#### 3.1 White Matter Structures

##### 3.1.1 Model Development

Association fiber FA was selected as the dependent variable for model development. The initial baseline model, which included only a random intercept for subjects, yielded an intraclass correlation coefficient (ICC) of .66, indicating about 66% of the variability in association fiber FA was between subjects and about 34% was within subjects.

Then, this null model was compared to a model that included the fixed effects of linear age, two intervention contrasts, and their interactions with linear age (i.e., linear age model). The linear age model had a significant improvement in fit,  $\chi^2(5) = 79.263, p < .001$ , supporting the inclusion of linear age and intervention effects.

Subsequently, the linear age model was compared to a model including main effects of linear age, quadratic age, two intervention contrasts, and their interactions with linear and quadratic age (i.e., quadratic age model). The quadratic age model had a significant improvement in fit,  $\chi^2(3) = 10.626, p = .014$ , suggesting that developmental changes in association FA were better captured by a nonlinear (quadratic) trajectory than a linear one.

To explore whether allowing individual differences in the rate of change over time would further improve model fit, a model with a random slope for linear age (in

addition to a random intercept) was evaluated. This model resulted in a boundary (singular) solution, where the random slope variance was close to zero. Consistent with this, the model comparison between the random-slope model and the quadratic model was not significant,  $\chi^2(2) = .066, p = .967$ . Therefore, due to the singularity and lack of improved fit, we opted to retain the simpler quadratic model with a random intercept for primary analyses.

Finally, we estimated a model with a random slope for quadratic age (in addition to a random intercept). This model also showed signs of singularity. In addition, the inclusion of a random effect of quadratic age did not significantly improve fit,  $\chi^2(2) = 4.128, p = .127$ . When both linear and quadratic random slopes were included, the model was overparameterized and failed to produce estimable variance components.

Taken together, the most parsimonious and best-fitting model was the quadratic model, which included both linear and quadratic fixed effects of age and their interactions with intervention, along with a random intercept for participants. This model was used for all subsequent hypothesis testing.

### **3.1.2 Association Fiber**

There were significant main effects of both linear and quadratic age, indicating that association fiber FA increased with age in a nonlinear trajectory for ABC. The contrast comparing the low-risk group to the ABC group was also significant, suggesting that, at the mean age, adolescents in the low-risk group exhibited higher overall FA than those in the ABC group. In contrast, the main effect comparing the DEF and ABC groups was not significant.

Significant interactions emerged between intervention group and quadratic age. Specifically, both the DEF versus ABC and the low-risk versus ABC contrasts interacted significantly with quadratic age, suggesting that the shape of developmental change in association fiber FA differed across groups. Adolescents in the DEF and low-risk groups showed a flatter trajectory in FA at later ages compared to those in the ABC group. In contrast, interactions between intervention group and linear age were not significant, indicating that the rate of FA change at the mean age did not differ significantly between groups. See Table 3 for full model estimates and Figure 3 for visualized trajectories.

Table 3. Fixed Effects for Association Fiber

Predictors	Estimates	Std. Error	<i>p</i> -Value
(Intercept)	.4892	.0027	<.001
Age	.0063	.0012	<.001
Age <sup>2</sup>	.0044	.0014	.001
DEF v ABC	.0040	.0038	.289
Low Risk v ABC	.0081	.0039	.039
Age x DEF v ABC	.0017	.0016	.309
Age x Low Risk v ABC	.0002	.0018	.908
Age <sup>2</sup> x DEF v ABC	-.0037	.0018	.042
Age <sup>2</sup> x Low Risk v ABC	-.0045	.0020	.023

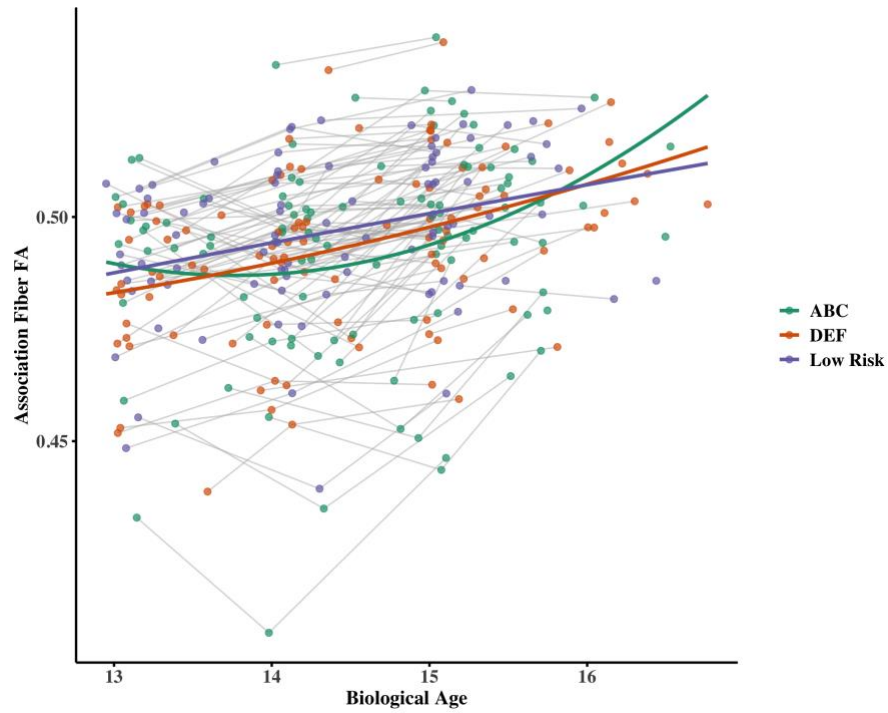


Figure 3. Association Fiber FA Trajectories by Intervention Groups. Spaghetti plot shows individual trajectories (thin grey lines) of FA across time (in years). Thick solid lines represent group-level fitted regression lines. ABC, DEF, and Low-Risk groups are shown in green, orange, and purple, respectively.

Additional models were tested that included random slopes for linear and quadratic age (see Table 4), but these did not alter the direction or significance of any effects.

Table 4. Fixed Effect Estimates Including Random Slope for Association Fibers

<i>Predictors</i>	Random Slope of Linear Age			Random Slope of Quadratic Age		
	<i>Estimates</i>	<i>std. Error</i>	<i>p</i>	<i>Estimates</i>	<i>std. Error</i>	<i>p</i>
Intercept	.489205	.002701	<.001	.489323	.002854	<.001
Age (linear, centered)	.006317	.001210	<.001	.006136	.001168	<.001
Age <sup>2</sup> (centered)	.004401	.001355	.001	.004103	.001320	.002
DEF v ABC	.004039	.003804	.289	.004172	.004013	.299
Low-Risk v ABC	.008076	.003896	.039	.008186	.004114	.048
Age × DEF v ABC	.001669	.001637	.309	.001820	.001573	.248
Age × Low-Risk	.000226	.001784	.899	.000279	.001718	.871
Age <sup>2</sup> × DEF v ABC	-.003663	.001796	.042	-.003704	.001747	.035
Age <sup>2</sup> × Low-Risk	-.004475	.001961	.023	-.004533	.001919	.019
<b>Random Effects</b>						
$\sigma^2$	0			0		
$\tau_{00}$	0.00 ChCode			0.00 ChCode		
$\tau_{11}$	0.00 ChCode.Age.Y			0.00 ChCode.Age.Y2		
$\rho_{01}$	-1.00 ChCode			-1.00 ChCode		
N	145 ChCode			145 ChCode		
Observations	300			300		
Marginal R <sup>2</sup> / Conditional R <sup>2</sup>	0.406 / NA			0.398 / NA		
Error	Singularity (variance is close to 0)			Singularity (variance is close to 0)		

### 3.1.3 Commissural Fiber

There were significant main effects of both linear and quadratic age, indicating that FA increased with age in a nonlinear trajectory for ABC. At the mean age, the contrast comparing the low-risk group to the ABC group showed a marginally significant main effect ( $p = .056$ ), suggesting a trend toward higher FA in the low-risk group relative to ABC. The main effect for the DEF versus ABC contrast was not significant.

Significant interactions emerged between intervention group and quadratic age. Specifically, both the DEF versus ABC and the low-risk versus ABC contrasts interacted significantly with quadratic age. These interactions indicated that developmental trajectories in commissural FA differed by group. Adolescents in the DEF and low-risk groups showed less pronounced nonlinear increases, possibly reflecting an earlier plateau or slower growth in FA at later ages, compared to those in the ABC group. In contrast, interactions between intervention group and linear age were not significant, indicating that the rate of FA change at the mean age did not differ significantly between groups. See Table 5 for full model estimates and Figure 4 for visualized trajectories.

Table 5. Fixed Effects for Commissural Fiber

Predictors	Estimates	Std. Error	<i>p</i> -Value
(Intercept)	.5734	.0029	<.001
Age	.0057	.0014	<.001
Age <sup>2</sup>	.0047	.0016	.003
DEF v ABC	.0056	.0041	.179

Low Risk v ABC	.0082	.0042	.056
Age x DEF v ABC	.0028	.0019	.142
Age x Low Risk v ABC	.0015	.0021	.473
Age <sup>2</sup> x DEF v ABC	-.0045	.0021	.030
Age <sup>2</sup> x Low Risk v ABC	-.0061	.0023	.008

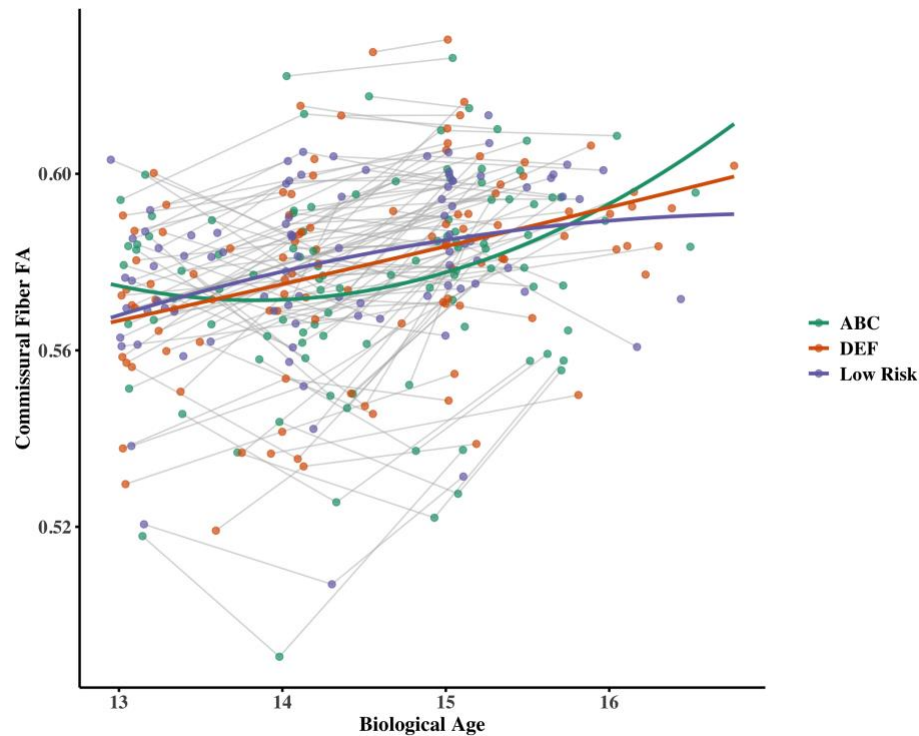


Figure 4. Commissural Fiber FA Trajectories by Intervention Groups. Spaghetti plot shows individual trajectories (thin grey lines) of FA across time (in years). Thick solid lines represent group-level fitted regression lines. ABC, DEF, and Low-Risk groups are shown in green, orange, and purple, respectively.

Additional models were tested that included random slopes for linear and quadratic age (see Table 6), but these did not alter the direction or significance of any effects.

Table 6. Fixed Effect Estimates Including Random Slope for Commissural Fibers

<i>Predictors</i>	Random Slope of Linear Age			Random Slope of Quadratic Age		
	<i>Estimates</i>	<i>std. Error</i>	<i>p</i>	<i>Estimates</i>	<i>std. Error</i>	<i>p</i>
Intercept	.573410	.002937	<.001	.573754	.003164	<.001
Age (linear, centered)	.005636	.001417	<.001	.005375	.001336	<.001
Age <sup>2</sup> (centered)	.004601	.001562	.003	.003990	.001497	.008
DEF v ABC	.005593	.004141	.178	.005358	.004450	.230
Low-Risk v ABC	.008117	.004242	.057	.008096	.004572	.078
Age × DEF v ABC	.002832	.001915	.140	.003030	.001795	.093
Age × Low-Risk	.001602	.002081	.442	.001526	.001957	.436
Age <sup>2</sup> × DEF v ABC	-.004531	.002064	.029	-.004191	.001978	.035
Age <sup>2</sup> × Low-Risk	-.006018	.002267	.008	-.005792	.002197	.009
<b>Random Effects</b>						
$\sigma^2$	0			0		
$\tau_{00}$	0.00 ChCode			0.00 ChCode		
$\tau_{11}$	0.00 ChCode.Age.Y			0.00 ChCode.Age.Y2		
$\rho_{01}$	-1.00 ChCode			-1.00 ChCode		
N	145 ChCode			145 ChCode		
Observations	300			300		
Marginal R <sup>2</sup> / Conditional R <sup>2</sup>	0.339 / NA			0.113 / 0.764		
Error	Singularity (variance is close to 0)			Singularity (variance is close to 0)		

### 3.1.4 Projection Fiber

Significant main effects of both linear and quadratic age emerged for the ABC group, indicating that FA increased with age in a nonlinear trajectory for ABC. At the mean age, the contrast comparing the low-risk group to ABC showed a marginally significant main effect ( $p = .096$ ), suggesting a trend toward higher FA in the low-risk group relative to ABC. The main effect for the DEF versus ABC contrast was not significant.

Significant interactions emerged between intervention group and quadratic age. Specifically, both the DEF versus ABC and low-risk versus ABC contrasts interacted significantly with quadratic age. These interactions indicate that developmental trajectories in projection FA differed by group. Adolescents in both the DEF and low-risk groups showed attenuated nonlinear increases, potentially reflecting a plateau or deceleration in FA growth at later ages, compared to those in the ABC group. In contrast, interactions between intervention group and linear age were not significant, indicating that the rate of FA change at the mean age did not differ significantly between groups. See Table 7 for full model estimates and Figure 5 for visualized trajectories.

Table 7. Fixed Effects for Projection Fiber

Predictors	Estimates	Std. Error	<i>p</i> -Value
(Intercept)	.5432	.0025	<.001
Age	.0062	.0013	<.001
Age <sup>2</sup>	.0045	.0014	.002
DEF v ABC	.0034	.0035	.341

Low Risk v ABC	.0061	.0036	.096
Age x DEF v ABC	.0014	.0017	.431
Age x Low Risk v ABC	.0005	.0019	.795
Age <sup>2</sup> x DEF v ABC	-.0037	.0019	.049
Age <sup>2</sup> x Low Risk v ABC	-.0045	.0021	.031

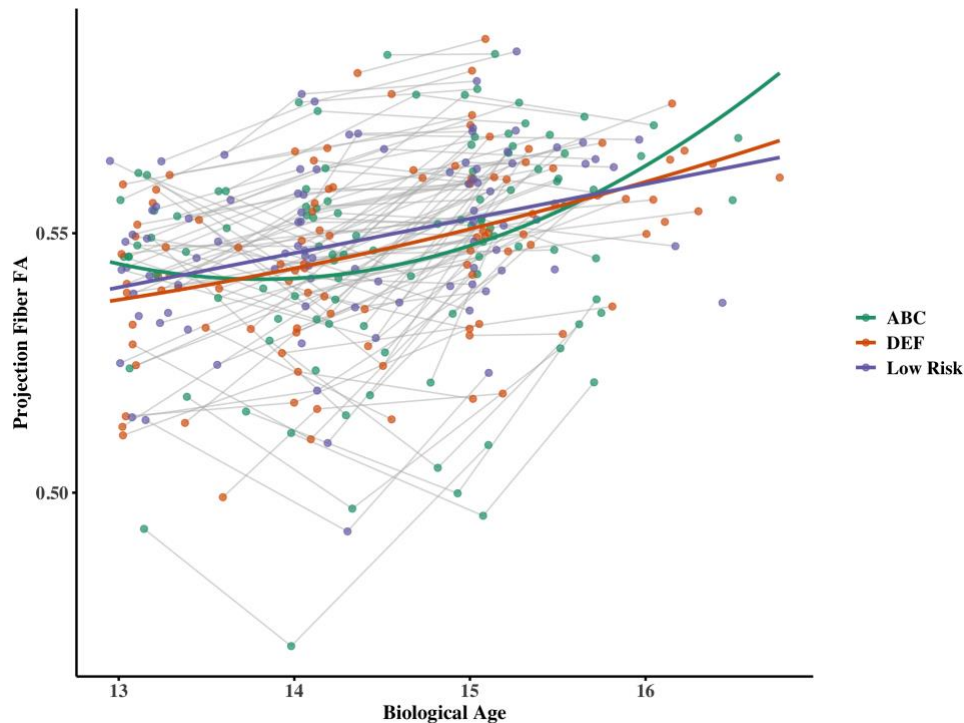


Figure 5. Projection Fiber FA Trajectories by Intervention Groups. Spaghetti plot shows individual trajectories (thin grey lines) of FA across time (in years). Thick solid lines represent group-level fitted regression lines. ABC, DEF, and Low-Risk groups are shown in green, orange, and purple, respectively.

Additional models were tested that included random slopes for linear and quadratic age (see Table 8), but these did not alter the direction or significance of any effects.

Table 8. Fixed Effect Estimates Including Random Slope for Projection Fibers

<i>Predictors</i>	Random Slope of Linear Age			Random Slope of Quadratic Age		
	<i>Estimates</i>	<i>std. Error</i>	<i>p</i>	<i>Estimates</i>	<i>std. Error</i>	<i>p</i>
Intercept	.543218	.002508	<.001	.543616	.002721	<.001
Age (linear, centered)	.006107	.001282	<.001	.005755	.001197	<.001
Age <sup>2</sup> (centered)	.004416	.001412	.002	.003827	.001328	.004
DEF v ABC	.003364	.003541	.343	.003394	.003830	.376
Low-Risk v ABC	.006042	.003629	.097	.006170	.003942	.119
Age × DEF v ABC	.001371	.001732	.429	.001741	.001607	.279
Age × Low-Risk	.000526	.001883	.780	.000484	.001748	.782
Age <sup>2</sup> × DEF v ABC	-.003673	.001866	.050	-.003547	.001755	.044
Age <sup>2</sup> × Low-Risk	-.004422	.002054	.032	-.004500	.001960	.022
<b>Random Effects</b>						
$\sigma^2$	0			0		
$\tau_{00}$	0.00 ChCode			0.00 ChCode		
$\tau_{11}$	0.00 ChCode.Age.Y			0.00 ChCode.Age.Y2		
$\rho_{01}$	-1.00 ChCode			-1.00 ChCode		
N	145 ChCode			145 ChCode		
Observations	300			300		
Marginal R <sup>2</sup> / Conditional R <sup>2</sup>	0.347 / NA			0.130 / 0.737		
Error	Singularity (variance is close to 0)			Singularity (variance is close to 0)		

### 3.1.5 Summary of Three Major White Matter Structures with FA

Given that the primary hypothesis concerned group differences in the nonlinear developmental trajectories of FA, the quadratic age by intervention interactions were treated as focal effects. To correct for multiple testing across all three major white matter structures, false discovery rate (FDR) correction was applied to the set of interaction terms involving quadratic age.

All six interaction terms (DEF versus ABC and low-risk versus ABC across the three fiber structures) remained significant after FDR correction (Table 9). These results support robust group differences in the shape of white matter development, particularly at later ages. These findings highlight meaningful and consistent differences in nonlinear white matter growth trajectories between ABC, DEF, and low-risk adolescents.

Table 9. FDR Correction for Quadratic Age by Group Effects

Fiber Type	Contrast	$\beta$ (Estimate)	<i>p</i> -Value	<i>p</i> (FDR)
Association	Age <sup>2</sup> × DEF v ABC	-.00368	.0421	.0488
Association	Age <sup>2</sup> × Low Risk v ABC	-.00451	.0228	.0474
Projection	Age <sup>2</sup> × DEF v ABC	-.00372	.0488	.0488
Projection	Age <sup>2</sup> × Low Risk v ABC	-.00446	.0316	.0474
Commissural	Age <sup>2</sup> × DEF v ABC	-.00455	.0303	.0474
Commissural	Age <sup>2</sup> × Low Risk v ABC	-.00608	.0084	.0474

## 3.2 Global Network Characteristics

### 3.2.1 Model Development

To determine the optimal model structure for predicting global network characteristics, we conducted a series of nested model comparisons using likelihood ratio tests and maximum likelihood (ML) estimation, consistent with the prior procedure conducted for white matter structures. Density was selected as the dependent variable for model development. The initial baseline model, which included only a random intercept for subjects, yielded an intraclass correlation coefficient (ICC) of .75, indicating about 75% of the variability in association fiber FA was between subjects and about 25% was within subjects.

We first compared a null model that included only a random intercept for subjects to a model that included linear age and intervention contrasts (i.e., DEF versus ABC and low-risk versus ABC), along with interaction terms between age and contrasts (i.e., linear age model). The linear age model showed significantly improved model fit compared to the null model,  $\chi^2(5) = 37.744$ ,  $p < .001$ , indicating age-related and group-related differences in density. Next, we evaluated whether adding a quadratic age term and its interactions improved model fit (i.e., quadratic age model). The model including quadratic age did not significantly outperform the linear age model,  $\chi^2(3) = 2.461$ ,  $p = .482$ , suggesting that the trajectory of network density was best captured by a linear rather than nonlinear age pattern.

Finally, we compared the linear age model to a version that included a random slope for age across subjects. This model failed to improve fit significantly,  $\chi^2(2) = 0.700$ ,  $p = .704$ , and produced a boundary (singular) fit, indicating insufficient variability in the random effect. Taken together, the linear age model with fixed slopes

and a random intercept was selected as the final model. This model was used for all subsequent hypothesis testing.

### 3.2.2 Density

A significant main effect of age emerged, indicating that network density decreased with age across the sample. However, neither the main effects of group (DEF versus ABC and low-risk versus ABC) nor the interaction terms with age were significant, indicating that the rate of age-related decline in network density did not differ significantly by intervention group. See Table 10 for full model estimates and Figure 6 for visualized trajectories.

Table 10. Fixed Effects for Density

Predictors	Estimates	Std. Error	<i>p</i> -Value
Intercept	.1441	.0017	<.001
Age	-.0025	.0009	.005
DEF v ABC	-.0010	.0024	.689
Low Risk v ABC	.0001	.0025	.957
Age × DEF v ABC	.0006	.0012	.636
Age × Low Risk v ABC	-.0016	.0013	.206

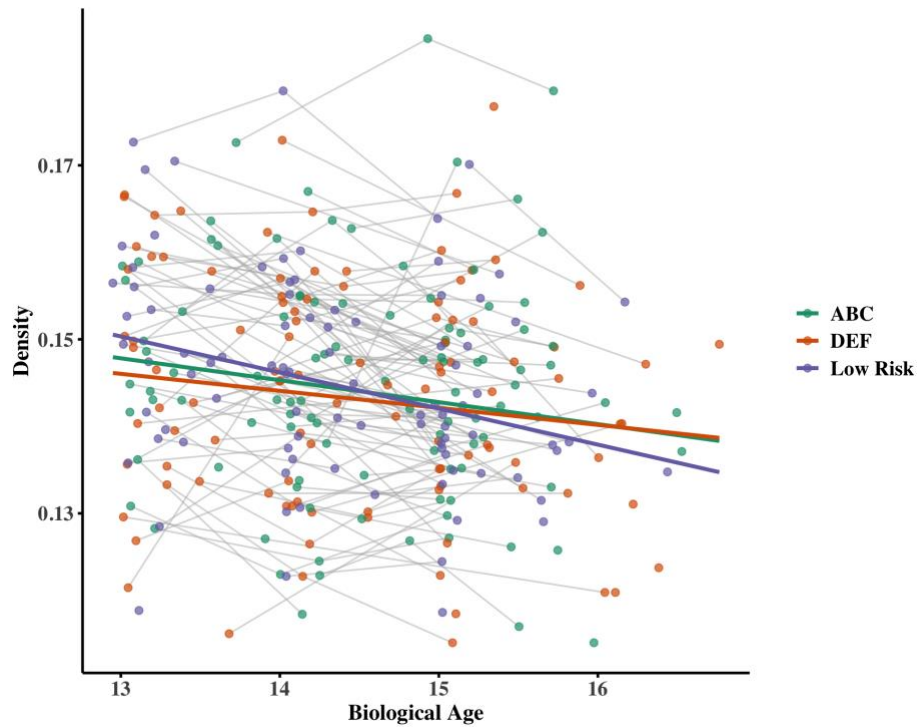


Figure 6. Density Trajectories by Intervention Groups. Spaghetti plot shows individual trajectories (thin grey lines) of density across time (in years). Thick solid lines represent group-level fitted regression lines. ABC, DEF, and Low-Risk groups are shown in green, orange, and purple, respectively.

### 3.2.3 Global Efficiency

There were no significant main effects of age or intervention group on global efficiency. However, a significant interaction between age and the low-risk versus ABC contrast emerged, indicating that the trajectory of global efficiency differed between the low-risk and ABC groups. Specifically, global efficiency declined more steeply with age in the low-risk group compared to the ABC group. No significant age by DEF versus ABC contrast interaction was found. Simple slope analyses were conducted to probe the age-related change in global efficiency within each group. For the ABC adolescents, the slope between age and global efficiency did not differ

significantly from zero ( $\beta = -.0002$ ,  $SE = .0005$ ,  $p = .608$ ). However, significant age-related decline was found among the DEF ( $\beta = -.001$ ,  $SE = .0004$ ,  $p < .001$ ) and low-risk adolescents ( $\beta = -.003$ ,  $SE = .0005$ ,  $p < .001$ ). See Table 11 for full model estimates and Figure 7 for visualized trajectories.

Table 11. Fixed Effects for Global Efficiency

Predictors	Estimates	Std. Error	<i>p</i> -Value
Intercept	.0405	.0012	<.001
Age	-.0002	.0005	.608
DEF v ABC	.0019	.0017	.272
Low Risk v ABC	.0024	.0018	.177
Age $\times$ DEF v ABC	-.0010	.0006	.100
Age $\times$ Low Risk v ABC	-.0023	.0007	.001

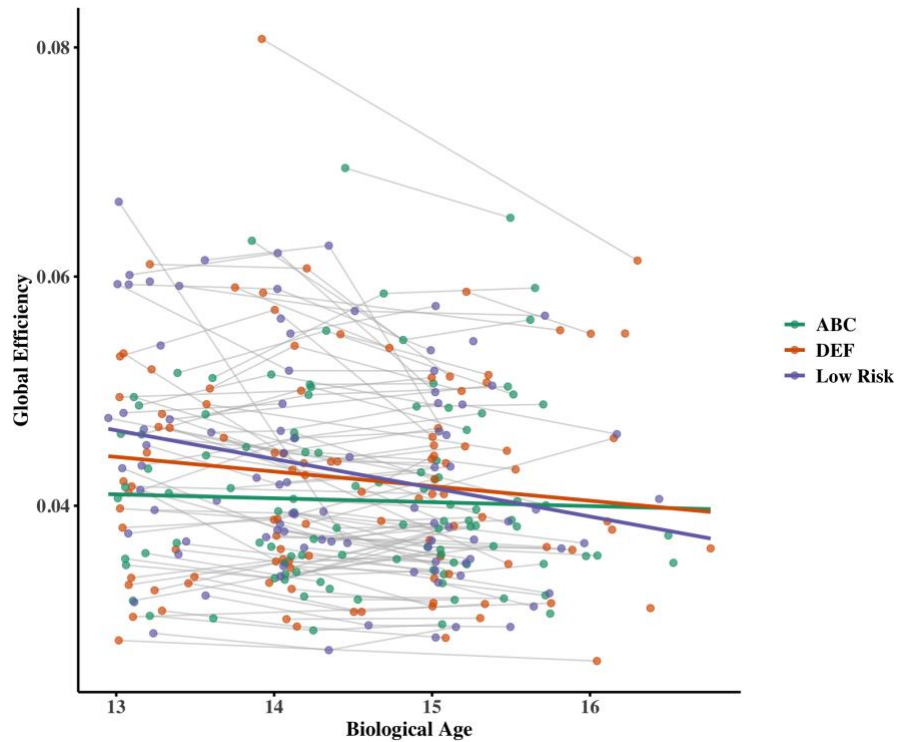


Figure 7. Global Efficiency Trajectories by Intervention Groups. Spaghetti plot shows individual trajectories (thin grey lines) of global efficiency across time (in years). Thick solid lines represent group-level fitted regression lines. ABC, DEF, and Low-Risk groups are shown in green, orange, and purple, respectively.

### 3.2.4 Small Worldness

There was no significant main effect of age or intervention group on small worldness. However, a significant interaction emerged between age and the low-risk versus ABC contrast, suggesting that the developmental trajectory of small worldness differed between these groups. Specifically, adolescents in the low-risk group showed a steeper age-related decline in small worldness relative to those in the ABC group. No such interaction was observed between age and the DEF versus ABC contrast. Simple slope analyses were conducted to probe the age-related change in small

worldness within each group. Among ABC adolescents, the slope between age and small worldness did not differ from zero ( $\beta = -.00000002$ ,  $SE = .000003$ ,  $p = .993$ ). However, significant age-related decline was found among low-risk adolescents ( $\beta = -.000008$ ,  $SE = .000003$ ,  $p = .004$ ). The slope for DEF adolescents was trending in the same direction as their low-risk peers but did not reach significance ( $\beta = -.000005$ ,  $SE = .000003$ ,  $p = .098$ ). See Table 12 for full model estimates and Figure 8 for visualized trajectories.

Table 12. Fixed Effects for Small Worldness

Predictors	Estimates	Std. Error	<i>p</i> -Value
Intercept	.0001315	.0000060	<.001
Age	.0000000	.0000028	.993
DEF v ABC	.0000049	.0000084	.558
Low Risk v ABC	.0000090	.0000087	.304
Age × DEF v ABC	-.0000049	.0000038	.202
Age × Low Risk v ABC	-.0000087	.0000041	.033

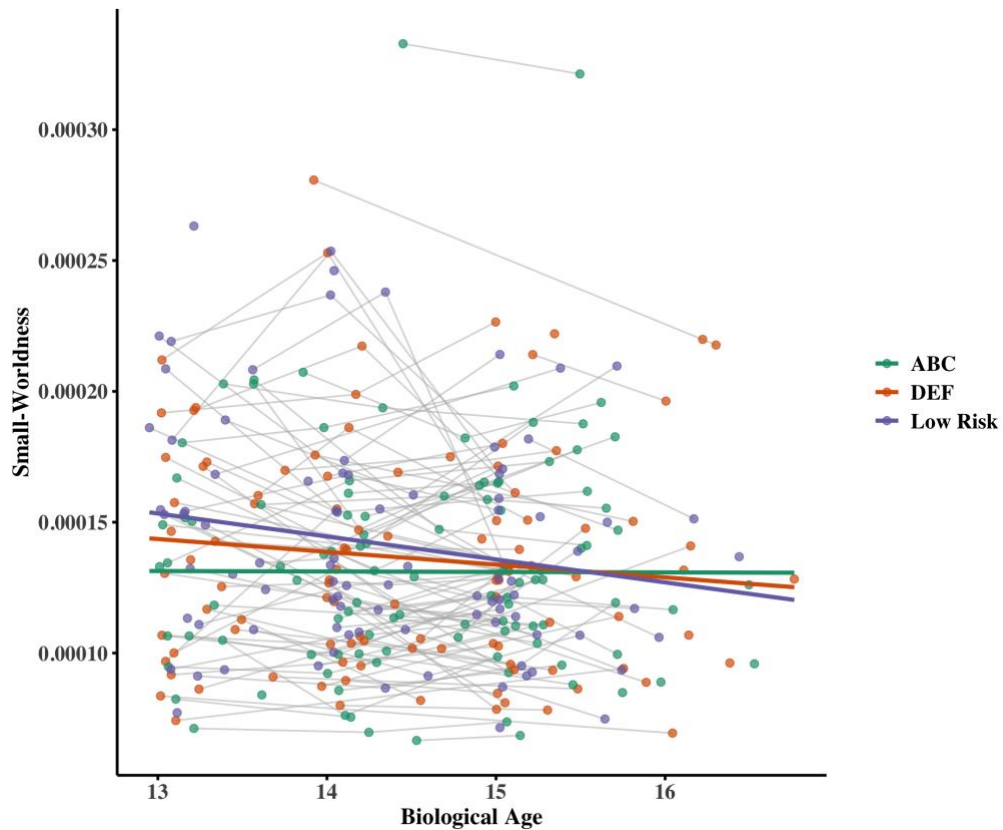


Figure 8. Small Worldness Trajectories by Intervention Groups. Spaghetti plot shows individual trajectories (thin grey lines) of small worldness across time (in years). Thick solid lines represent group-level fitted regression lines. ABC, DEF, and Low-Risk groups are shown in green, orange, and purple, respectively.

### 3.3 Post-Hoc Analyses on White Matter Structures with Mean Diffusivity

#### 3.3.1 Association Fiber

There was a significant main effect of linear but not quadratic age, indicating that association fiber MD increased with age in a linear trajectory for ABC. At the mean age, the contrast comparing DEF to ABC showed a significant main effect ( $p = .003$ ), suggesting that adolescents in the DEF exhibited higher overall MD than those

in the ABC group. In addition, the contrast between low-risk and ABC groups showed a marginally significant main effect ( $p = .052$ ), suggesting a trend toward higher MD in the low-risk group relative to ABC. However, no significant interactions were detected between intervention group and quadratic age or between intervention group and linear age. Adolescents across all three groups demonstrated increased MD with age, though those in the ABC group increased at a slower rate than the other two groups. Contrast coding was modified to examine the shape of the trajectory for the DEF and low-risk groups. When DEF is the reference group, there were significant main effects for both linear ( $\beta = .000021$ ,  $SE = .000002$ ,  $p = <.001$ ) and quadratic ( $\beta = -.000008$ ,  $SE = .000002$ ,  $p = .001$ ) age, indicating that association fiber MD increased with age in a nonlinear trajectory. In addition, when the low-risk group was included as the reference group, there were significant main effects for both linear ( $\beta = .000020$ ,  $SE = .000003$ ,  $p = <.001$ ) and quadratic ( $\beta = -.000006$ ,  $SE = .000003$ ,  $p = .042$ ) age, indicating that association fiber MD increased with age in a nonlinear trajectory. See Table 13 for full model estimates with ABC as the reference group and Figure 9 for visualized trajectories.

Table 13. Fixed Effects for Association Fiber

Predictors	Estimates	Std. Error	<i>p</i> -Value
(Intercept)	.000730	.000004	<0.001
Age	.000023	.000003	<0.001
Age <sup>2</sup>	-.000002	.000003	.405
DEF v ABC	.000016	.000005	.003
Low Risk v ABC	.000011	.000006	.052
Age x DEF v ABC	-.000001	.000003	.687

Age x Low Risk v ABC	-.000002	.000004	.593
Age <sup>2</sup> x DEF v ABC	-.000005	.000004	.136
Age <sup>2</sup> x Low Risk v ABC	-.000004	.000004	.351

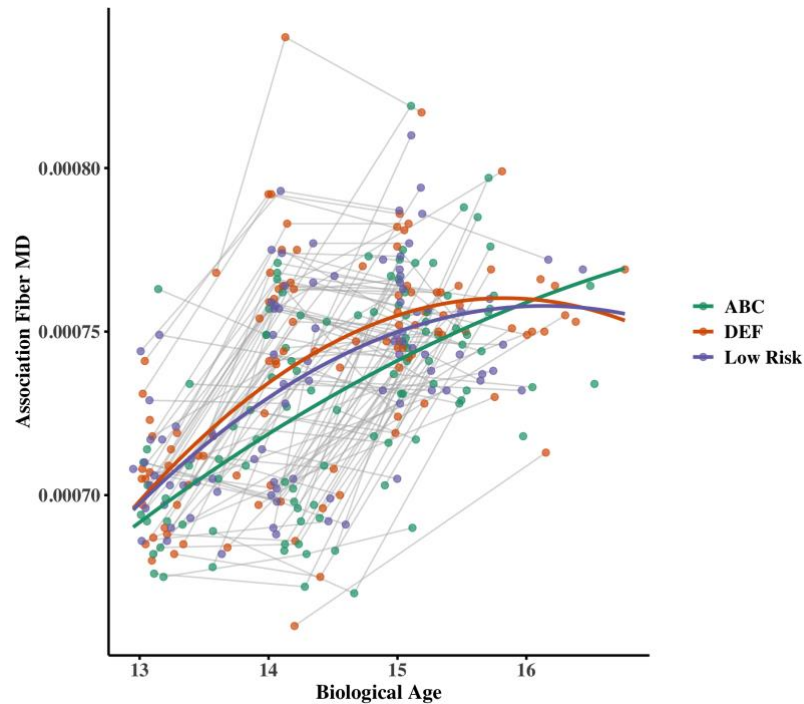


Figure 9. Association Fiber MD Trajectories by Intervention Groups. Spaghetti plot shows individual trajectories (thin grey lines) of MD across time (in years). Thick solid lines represent group-level fitted regression lines. ABC, DEF, and Low-Risk groups are shown in green, orange, and purple, respectively.

### 3.3.2 Commissural Fiber

There was a significant main effect of linear but not quadratic age, indicating that commissural fiber MD increased with age in a linear trajectory for ABC. At the mean age, the contrast comparing DEF to ABC showed a significant main effect ( $p = .039$ ), indicating that adolescents in the DEF exhibited higher overall MD than those

in the ABC group. In contrast, no significant main effect was detected when comparing low-risk group to ABC. In addition, no significant interactions were detected between intervention group and quadratic age or between intervention group and linear age. Adolescents across all three groups demonstrated increased MD with age, though those in the ABC group increased at a slower rate than the other two groups. When DEF was included as the reference group, there were significant main effects for both linear ( $\beta = .000027$ ,  $SE = .000003$ ,  $p = <.001$ ) and quadratic ( $\beta = -.000008$ ,  $SE = .000003$ ,  $p = .007$ ) age, indicating that commissural fiber MD increased with age in a nonlinear trajectory. In addition, when low-risk group was included as the reference group, there were significant main effects for both linear ( $\beta = .000027$ ,  $SE = .000003$ ,  $p = <.001$ ) and quadratic ( $\beta = -.000008$ ,  $SE = .000004$ ,  $p = .042$ ) age, indicating that commissural fiber MD increased with age in a nonlinear trajectory. See Table 14 for full model estimates with ABC as the reference group and Figure 10 for visualized trajectories.

Table 14. Fixed Effects for Commissural Fiber

Predictors	Estimates	Std. Error	<i>p</i> -Value
(Intercept)	0.000752	0.000005	<0.001
Age	0.000028	0.000003	<0.001
Age <sup>2</sup>	-0.000003	0.000003	0.349
DEF v ABC	0.000013	0.000006	0.039
Low Risk v ABC	0.000009	0.000007	0.199
Age x DEF v ABC	-0.000001	0.000004	0.769
Age x Low Risk v ABC	-0.000002	0.000005	0.732
Age <sup>2</sup> x DEF v ABC	-0.000005	0.000004	0.296

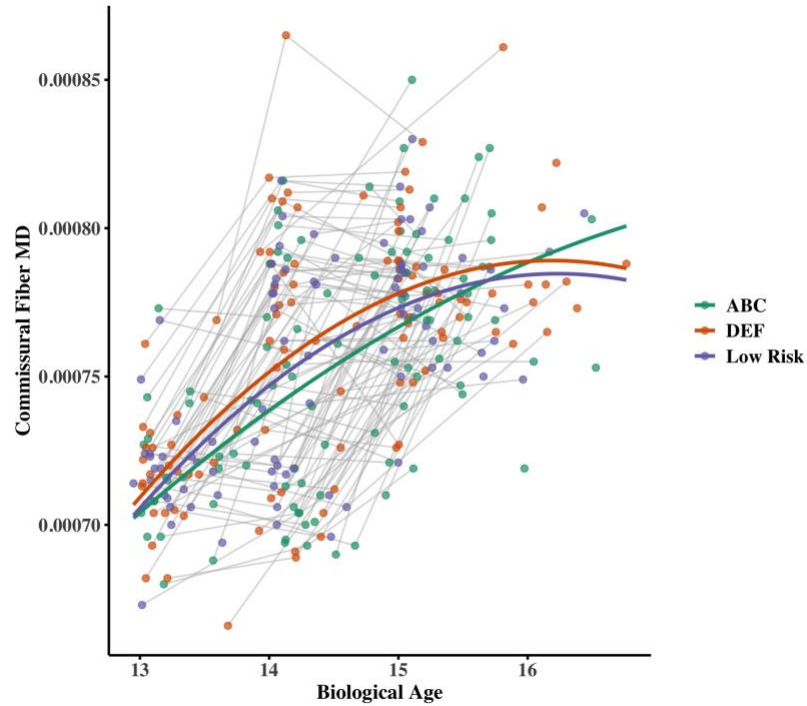


Figure 10. Commissural Fiber MD Trajectories by Intervention Groups. Spaghetti plot shows individual trajectories (thin grey lines) of MD across time (in years). Thick solid lines represent group-level fitted regression lines. ABC, DEF, and Low-Risk groups are shown in green, orange, and purple, respectively.

### 3.3.3 Projection Fiber

There was a significant main effect of linear but not quadratic age, indicating that projection fiber MD increased with age in a linear trajectory for ABC. At the mean age, the contrast comparing DEF to ABC showed a significant main effect ( $p = .004$ ), suggesting that adolescents in the DEF exhibited higher overall MD than those in the ABC group. In addition, the contrast comparing low-risk group to ABC also

showed a significant main effect ( $p = .041$ ), suggesting that those in the low-risk group exhibited higher MD than ABC counterparts. However, no significant interactions were detected between intervention group and quadratic age or between intervention group and linear age. Adolescents across all three groups demonstrated increased MD with age, though those in the ABC group increased at a slower rate than the other two groups. When DEF was included as the reference group, there were significant main effects for both linear ( $\beta = .000023$ ,  $SE = .000002$ ,  $p = <.001$ ) and quadratic ( $\beta = -.000008$ ,  $SE = .000002$ ,  $p = .002$ ) age, indicating that projection fiber MD increased with age in a nonlinear trajectory. In contrast, when low-risk group was included as the reference group, there was a significant main effect for linear age ( $\beta = .000023$ ,  $SE = .000003$ ,  $p = <.001$ ). There was a marginally significant main effect for quadratic age ( $\beta = -.000006$ ,  $SE = .000003$ ,  $p = .054$ ). Together, these results indicate that projection fiber MD increased with age in a linear trajectory with a trend towards a curvilinear pattern. See Table 15 for full model estimates with ABC as the reference group and Figure 11 for visualized trajectories.

Table 15. Fixed Effects for Projection Fiber

Predictors	Estimates	Std. Error	<i>p</i> -Value
(Intercept)	0.000697	0.000004	<0.001
Age	0.000025	0.000003	<0.001
Age <sup>2</sup>	-0.000003	0.000003	0.287
DEF v ABC	0.000015	0.000005	0.004
Low Risk v ABC	0.000011	0.000005	0.041
Age x DEF v ABC	-0.000002	0.000004	0.575
Age x Low Risk v ABC	-0.000002	0.000004	0.574

Age <sup>2</sup> x DEF v ABC	-0.000005	0.000004	0.227
Age <sup>2</sup> x Low Risk v ABC	-0.000003	0.000004	0.483

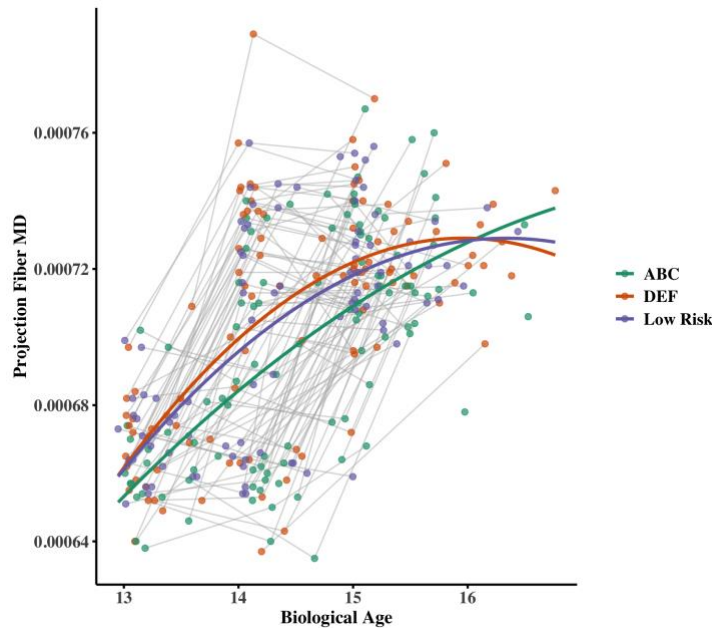


Figure 11. Projection Fiber MD Trajectories by Intervention Groups. Spaghetti plot shows individual trajectories (thin grey lines) of MD across time (in years). Thick solid lines represent group-level fitted regression lines. ABC, DEF, and Low-Risk groups are shown in green, orange, and purple, respectively.

### 3.3.4 Summary of Post-Hoc Analyses on Three Major White Matter Structures with MD

Post-hoc analyses of mean diffusivity across association, commissural, and projection fibers showed a consistent pattern of age-related increases in MD across groups. Notably, ABC adolescents demonstrated slower rates of increases (a steadily increasing, linear trajectory) than the DEF or low-risk group (a curvilinear trajectory that accelerated early, followed by deceleration at later ages). In addition, those in the

DEF consistently exhibited higher MD than their ABC counterparts across all three fiber structures. Although the low-risk adolescents generally showed higher MD than those in ABC, the findings were not as consistent as the comparison between DEF and ABC (with projection fiber reaching statistical significance only). There was no significant group-by-linear or quadratic age interaction.

### **3.4 Exploratory Analysis of Individual White Matter Fasciculi**

To identify specific white matter fasciculi showing differential age-related changes in FA across intervention groups, we conducted an exploratory analysis testing the interaction between intervention group and quadratic age ( $Age^2$ ) across 43 anatomically distinct fasciculi, made up of association, commissural, and projection fibers.

To control for multiple comparisons,  $p$ -values for all 86 interaction terms (43 \* 2 contrast interaction terms) were corrected using FDR. After correction, three fasciculi remained significant for the DEF versus ABC contrast: anterior thalamic radiation (right), dorsal cingulum (right), and forceps minor. For the low-risk versus ABC contrast, four fasciculi survived FDR correction: anterior thalamic radiation (right), perigenual cingulum (right), forceps minor, and middle longitudinal fasciculus (right). See Table 16 for full details.

Table 16. Exploratory Analysis of Individual White Matter Fasciculi

Outcome	Estimate	Std.Error	t-Value	df	p-Value	p(FDR)
Acoustic Radiation L	-.0031	.0024	-1.3334	244.7012	.1836	.2529
Acoustic Radiation R	-.0032	.0021	-1.5185	227.6804	.1303	.1990
Anterior Commissure	-.0064	.0036	-1.7713	190.9100	.0781	.1562
Anterior Thalamic Radiation L	-.0059	.0022	-2.6890	237.9722	.0077	.0579
Anterior Thalamic Radiation R	-.0060	.0020	-2.9465	235.0624	.0035	.0424
Arcuate Fasciculus L	-.0020	.0019	-1.0146	222.5824	.3114	.3583
Arcuate Fasciculus R	-.0030	.0017	-1.8061	203.1709	.0724	.1562
Cingulum Dorsal L	-.0060	.0022	-2.7650	217.2693	.0062	.0539
Cingulum Dorsal R	-.0065	.0020	-3.2516	196.6915	.0014	.0362
Cingulum Perigenual L	-.0033	.0032	-1.0218	241.7048	.3079	.3583
Cingulum Perigenual R	-.0016	.0027	-.6004	246.6665	.5488	.5488
Cingulum Temporal L	-.0081	.0034	-2.3520	247.9364	.0195	.0817
Cingulum Temporal R	-.0056	.0038	-1.4560	243.9229	.1467	.2162
Corticospinal Tract L	-.0039	.0023	-1.7427	253.4136	.0826	.1562
Corticospinal Tract R	-.0040	.0021	-1.8769	241.4688	.0617	.1467
Forceps Major	-.0015	.0022	-.7051	240.9256	.4814	.5062
Forceps Minor	-.0088	.0026	-3.3663	227.9576	.0009	.0362
Fornix L	-.0032	.0025	-1.2957	222.7412	.1964	.2599
Fornix R	-.0023	.0026	-.8750	212.1861	.3826	.4285

Frontal Aslant Tract L	-0.0026	.0018	-1.4664	216.4473	.1440	.2160
Frontal Aslant Tract R	-0.0043	.0017	-2.5012	219.1403	.0131	.0704
Inferior Fronto-Occipital Fasciculus L	-0.0032	.0024	-1.3188	236.4866	.1885	.2554
Inferior Fronto-Occipital Fasciculus R	-0.0018	.0019	-.9607	212.0131	.3378	.3834
Inferior Longitudinal Fasciculus L	-0.0057	.0032	-1.7478	262.2748	.0817	.1562
Inferior Longitudinal Fasciculus R	-0.0037	.0029	-1.2816	260.8662	.2011	.2599
Middle Cerebellar Peduncle	-0.0017	.0025	-.6716	249.3719	.5025	.5147
Middle Longitudinal Fasciculus L	-0.0026	.0022	-1.1920	225.0591	.2345	.2855
Middle Longitudinal Fasciculus R	-0.0013	.0019	-.6834	213.3993	.4951	.5134
Optic Radiation L	-0.0018	.0024	-.7418	239.4460	.4589	.4942
Optic Radiation R	-0.0022	.0022	-1.0153	226.4515	.3110	.3583
Superior Longitudinal Fasciculus 1 L	-0.0039	.0017	-2.2232	208.2568	.0273	.0924
Superior Longitudinal Fasciculus 1 R	-0.0028	.0017	-1.6404	212.9741	.1024	.1756
Superior Longitudinal Fasciculus 2 L	-0.0031	.0016	-1.8907	197.5561	.0601	.1467
Superior Longitudinal Fasciculus 2 R	-0.0043	.0018	-2.4347	203.3174	.0158	.0736
Superior Longitudinal Fasciculus 3 L	-0.0021	.0018	-1.1999	209.9913	.2315	.2855
Superior Longitudinal Fasciculus 3 R	-0.0041	.0017	-2.4847	204.0965	.0138	.0704
Superior Thalamic Radiation L	-0.0032	.0018	-1.8038	234.2156	.0725	.1562
Superior Thalamic Radiation R	-0.0041	.0019	-2.1584	236.5149	.0319	.0924
Uncinate Fasciculus L	-0.0028	.0023	-1.2341	250.5540	.2183	.2779
Uncinate Fasciculus R	-0.0044	.0026	-1.6773	252.5608	.0947	.1693
Vertical Occipital Fasciculus L	-0.0034	.0021	-1.6243	237.0853	.1056	.1775
Vertical Occipital Fasciculus R	-0.0045	.0022	-2.0534	238.5097	.0411	.1151

Age<sup>2</sup> x Low Risk v ABC

Outcome	Estimate	Std.Error	t-Value	df	p-Value	p(FDR)
Acoustic Radiation L	-.0028	.0026	-1.0743	227.1308	.2838	.3406
Acoustic Radiation R	-.0065	.0023	-2.8173	212.0002	.0053	.0539
Anterior Commissure	-.0090	.0039	-2.3088	181.5711	.0221	.0843
Anterior Thalamic Radiation L	-.0044	.0024	-1.8337	220.8915	.0680	.1545
Anterior Thalamic Radiation R	-.0071	.0022	-3.1736	218.7508	.0017	.0362
Arcuate Fasciculus L	-.0013	.0021	-.6370	207.8556	.5248	.5312
Arcuate Fasciculus R	-.0039	.0018	-2.1649	192.0664	.0316	.0924
Cingulum Dorsal L	-.0052	.0024	-2.1896	202.4045	.0297	.0924
Cingulum Dorsal R	-.0050	.0021	-2.3149	186.0869	.0217	.0843
Cingulum Perigenual L	-.0054	.0035	-1.5393	223.9004	.1251	.1983
Cingulum Perigenual R	-.0090	.0030	-2.9961	228.9544	.0030	.0424
Cingulum Temporal L	-.0066	.0038	-1.7269	230.2704	.0855	.1562
Cingulum Temporal R	-.0059	.0042	-1.3959	226.0967	.1641	.2337
Corticospinal Tract L	-.0043	.0025	-1.7298	236.5987	.0850	.1562
Corticospinal Tract R	-.0044	.0023	-1.8695	224.8342	.0629	.1467
Forceps Major	-.0032	.0024	-1.3594	224.2532	.1754	.2455
Forceps Minor	-.0099	.0029	-3.4586	212.2419	.0007	.0362
Fornix L	-.0052	.0027	-1.9283	207.8934	.0552	.1433
Fornix R	-.0043	.0028	-1.5275	198.4888	.1282	.1990
Frontal Aslant Tract L	-.0037	.0019	-1.9198	202.3216	.0563	.1433
Frontal Aslant Tract R	-.0046	.0019	-2.4722	204.7776	.0142	.0704
Inferior Fronto-Occipital Fasciculus L	-.0034	.0027	-1.2885	220.0025	.1989	.2599
Inferior Fronto-Occipital Fasciculus R	-.0057	.0021	-2.7551	198.8499	.0064	.0539
Inferior Longitudinal Fasciculus L	-.0025	.0036	-.7040	245.1269	.4821	.5062

Inferior Longitudinal Fasciculus R	-.0027	.0032	-.8394	243.9764	.4021	.4444
Middle Cerebellar Peduncle	-.0046	.0028	-1.6434	232.0833	.1017	.1756
Middle Longitudinal Fasciculus L	-.0029	.0024	-1.2193	210.0243	.2241	.2809
Middle Longitudinal Fasciculus R	-.0060	.0020	-2.9655	200.3986	.0034	.0424
Optic Radiation L	-.0021	.0026	-.8075	222.7832	.4202	.4584
Optic Radiation R	-.0057	.0024	-2.4138	210.8104	.0166	.0736
Superior Longitudinal Fasciculus 1 L	-.0050	.0019	-2.6677	195.3851	.0083	.0579
Superior Longitudinal Fasciculus 1 R	-.0041	.0019	-2.2115	200.1282	.0281	.0924
Superior Longitudinal Fasciculus 2 L	-.0045	.0018	-2.5399	187.2637	.0119	.0704
Superior Longitudinal Fasciculus 2 R	-.0051	.0019	-2.6296	191.8919	.0092	.0597
Superior Longitudinal Fasciculus 3 L	-.0030	.0019	-1.5684	197.5212	.1184	.1945
Superior Longitudinal Fasciculus 3 R	-.0039	.0018	-2.1965	192.6864	.0293	.0924
Superior Thalamic Radiation L	-.0028	.0020	-1.4340	218.2293	.1530	.2216
Superior Thalamic Radiation R	-.0041	.0021	-1.9540	220.3195	.0520	.1408
Uncinate Fasciculus L	-.0044	.0025	-1.7574	233.1030	.0802	.1562
Uncinate Fasciculus R	-.0065	.0029	-2.2675	234.7099	.0243	.0886
Vertical Occipital Fasciculus L	-.0035	.0023	-1.5592	219.6711	.1204	.1945
Vertical Occipital Fasciculus R	-.0042	.0024	-1.7456	221.5304	.0823	.1562

*Note:* L indicates left; R indicates right.

## Chapter 4

### DISCUSSION

The present study leveraged a longitudinal follow-up study of an RCT to investigate alterations of white matter microstructure and global network architecture during adolescence. In the RCT, parents involved with CPS due to maltreatment risk were randomly assigned to receive the ABC intervention or a control intervention, DEF, when their infants were under 24 months old. Approximately 11 years later, these adolescents underwent dMRI scans at ages 13, 14, and 15. A comparison group of adolescents with no previous CPS involvement, suggesting low risk of maltreatment, was also included in the analyses. We examined whether improving parenting quality through an early parenting intervention causally influenced the developmental trajectories of FA in three major white matter fiber structures, including association, commissural, and projection fiber (**Aim 1**), and global network characteristics, including density, global efficiency, and small worldness (**Aim 2**). Biological age was considered a continuous variable. Group differences over time were probed via testing the interactive effects between age and group using mixed-effects modeling. Post-hoc analyses on mean diffusivity (MD) were performed to complement the interpretation of FA results. Exploratory analyses were conducted to probe the interactive effects at the fasciculus level.

#### **4.1 Group Differences in the Developmental Trajectory of White Matter Fiber Structures**

We hypothesized that ABC adolescents would demonstrate a nonlinear age-related change in three major white matter fiber structures during adolescence, and that this pattern of change would differ from the pattern seen for DEF adolescents. Results indicated that FA increased with age following a quadratic trajectory for ABC adolescents. In addition, a significant quadratic age by group interaction emerged, where those in ABC demonstrated an initial decrease in FA (i.e., deceleration of growth velocity) followed by a later increase in FA (i.e., acceleration of growth velocity), while those in the DEF and low-risk groups exhibited a steady increase in FA over time (i.e., at a constant speed with little changes in growth velocity). In the post-hoc analyses, significant age-related increases in MD were observed across the three groups. While no significant age by group interactions emerged, there were qualitative differences between groups. The developmental trajectory of MD was better captured by a linear increase than a quadratic one for ABC adolescents. In contrast, for those in the DEF and low-risk groups, their trajectories were better described by a quadratic change, where the speed of MD increase decelerated, than by a linear one. To interpret these developmental patterns, the covarying changes in FA and MD were considered simultaneously. See Figure 12 for an illustrated interpretation.

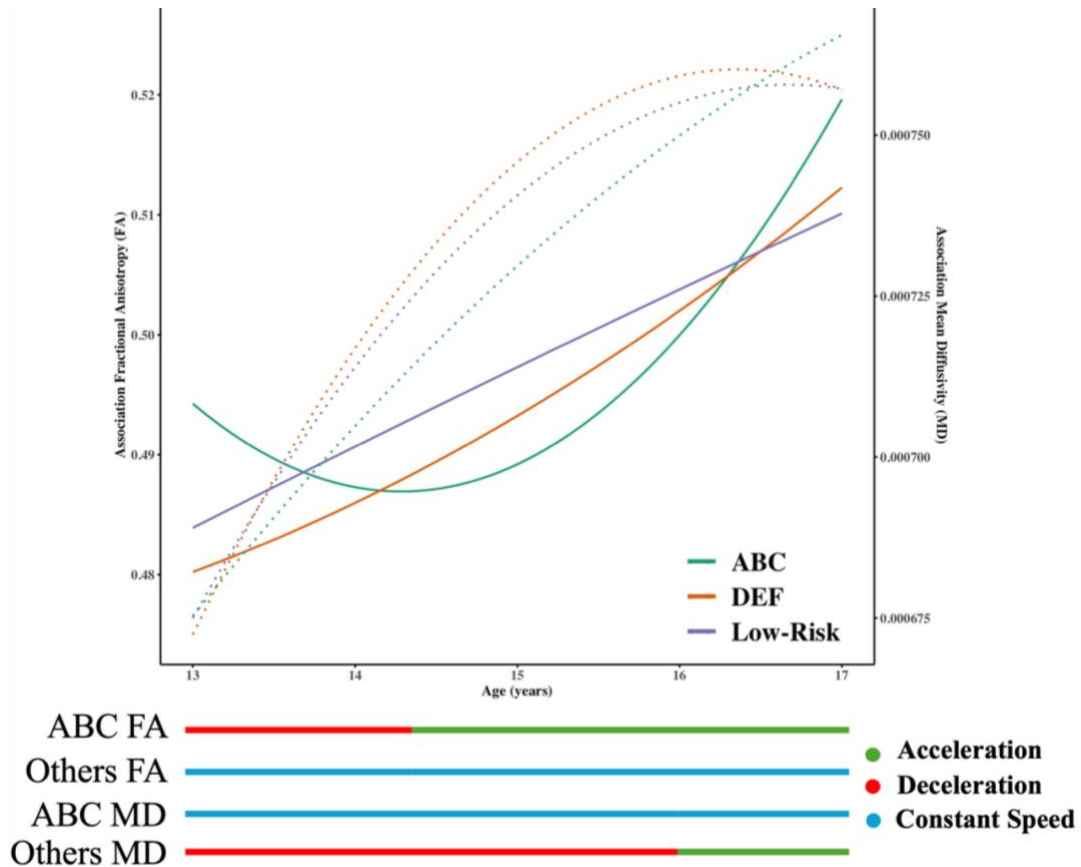


Figure 12. Predicted FA and MD Trajectories by Group. This figure illustrates the differences in developmental patterns between groups. Solid lines represent FA growth trajectories, and the dotted lines represent MD growth trajectories.

Both the DEF and low-risk groups exhibited a pattern of steady increases in FA and a nonlinear increase in MD, characterized by initial deceleration followed by acceleration in growth velocity. The literature suggests that prior to myelination, the adolescent brain undergoes axonal reorganization to enhance fiber coherence (Lebel & Beaulieu, 2011; Simmonds et al., 2014). This reorganization of axons involves eliminating inefficient pathways to promote fiber coherence, which in turn facilitates increased communicative efficiency through myelination. Indeed, the increases in both

FA and MD across major white matter fiber structures in both the DEF and low-risk groups likely reflect a fiber reorganization process. Moreover, both groups exhibited a decelerated pattern of MD increases, and as they reached later ages, the two groups began to show an accelerated pattern of decreasing MD. This dynamic pattern of MD changes, along with a linear increase in FA, suggests that the brain is undergoing the myelination process as adolescents in the DEF and low-risk groups become older. Studies have shown that the rapid increase in myelination during adolescence is a feature of white matter maturation, which, in contrast, demonstrates limited neuroplasticity for future experience-dependent development (Casey et al., 2025; Lebel et al., 2017).

Conversely, the ABC group exhibited a pattern of initial deceleration in FA (FA decreases, a “dip” phase in the trajectory), followed by acceleration in growth velocity (FA increases, a “recovery” phase in the trajectory). This pattern of FA changes occurred in the context of a linear increase in MD and minimal changes to growth velocity. A decrease in FA and an increase in MD among developing children have been described as signs of ongoing axonal remodeling, during which the proliferation of axons (in the context of crossing fibers) and fiber reorganization occur (Baker et al., 2025; Lebel et al., 2017). ABC adolescents “caught up” with the other group when FA increased with an accelerated velocity at later ages. Interestingly, the increases in FA among ABC adolescents coincided with a steady, linear increase in MD, rather than a decrease in MD. Typically, an increase in FA during adolescence is interpreted as a myelination process, without considering other complementary microstructural information, such as MD. However, myelination is marked by an inverse association between FA and MD, where FA increases and MD decreases, and

vice versa for de-myelination and edema. This association occurs because, in the presence of myelin, water diffusivity is restricted by the lipid-rich barrier. Inherently, when the white matter tissue is filled with myelin, there is limited extracellular space and diffusional freedom in the tissue. Within the ABC group at older ages, this pattern of increases in FA and MD likely reflects the reorganization process of white matter fibers, which is also seen in both the DEF and low-risk groups at earlier ages. Together, ABC adolescents appeared to show a more protracted development in white matter relative to those in the other groups. This pattern of protracted development has been described as an evolutionarily adaptive extension of neuroplasticity, where the developing brain remains malleable for later experience-dependent development (Casey et al., 2025; Lebel et al., 2017; Sampaio-Baptista & Johansen-Berg, 2017). In contrast, the DEF and low-risk groups appeared to demonstrate a more accelerated but time-limited pattern of maturation relative to ABC.

#### **4.2 Maltreatment-Specific Differences in the Developmental Trajectory of Global Network Characteristics**

Across groups, network density declined linearly with age, consistent with the normative neurodevelopmental process marked by decreased axonal packing and synaptic pruning (Fair et al., 2009). There were no significant group by age differences in either the intercept or the slope, suggesting that structural refinement may proceed similarly regardless of early parenting context. However, group by age differences emerged in the trajectories of global efficiency and small worldness. Specifically, low-risk adolescents exhibited significantly steeper age-related declines in both metrics compared to ABC youth, while ABC youth showed no significant age-

related change in either global network property. The DEF group did not differ significantly from either ABC or low-risk groups on these metrics.

Global efficiency and small worldness indicate the integration of large-scale networks and the balance between localized specialization and distributed information processing. Our findings suggest that ABC adolescents did not show age-related changes across time. Typically, global efficiency and small worldness increase with age to promote modularity and functional specialization (Whitaker et al., 2016). From this perspective, the preservation of global efficiency and small worldness in ABC adolescents may reflect a sustained neuroplasticity for integration and flexible communication across brain networks, potentially supporting adaptive functioning in the context of early adversity. In contrast, the steeper declines observed in DEF and low-risk adolescents may indicate earlier maturation of functional network organization.

### **4.3 Group Differences in Neuroplasticity**

According to the stress acceleration hypothesis (Callaghan & Tottenham, 2016), early adversity may speed up brain development. This accelerated process is posited to enable children to adapt to environments that are threatening, depriving, or unpredictable. However, the accelerated maturation is at the expense of limited neuroplasticity later in life. Our findings, especially the slower white matter development in ABC relative to DEF, are congruent with the stress acceleration hypothesis, where improvement in early parenting practices remediates the neurodevelopmental tempo that otherwise would lead to acceleration of maturation, as seen in the DEF group. In the context of an RCT, both ABC and DEF children had experienced parenting-related early adversity prior to randomization. Our findings that

adolescents in the ABC group showed more protracted white matter development relative to DEF indicate that early sensitive parenting may restore or even expand neurodevelopmental flexibility for children who experienced parenting-related adversity. These differences in developmental patterns appeared across various fiber structures, showing that early parenting has a global effect on the development of white matter.

During adolescence, the brain undergoes major cortical changes, including synaptic pruning and thinning of grey matter. This reorganization is salient in the prefrontal and temporal cortices (Giedd et al., 1999; Mills et al., 2016). These changes can temporarily disrupt nearby white matter systems, likely causing short-term declines in FA as pathways become unstable before they strengthen and stabilize. Adolescence also involves changes in inhibitory activity, with growing GABA signaling that shapes developing circuits (Caballero & Tseng, 2016). In this context, the FA “dip” seen in ABC adolescents may represent a phase of recalibration. The MD results clarify this pattern further. While FA in the ABC group showed a nonlinear trajectory, MD increased steadily and linearly, which is different than the early sharp increase seen in the DEF and low-risk groups. This suggests that ABC adolescents experienced dynamic changes in their brain structure in a more methodical, organized way than their DEF and low-risk peers, which consequently allows for an extended period of neuroplasticity, rather than haphazardly adapting to the suboptimal environment to maximize survival. Although this speculation about the different developmental patterns between ABC and DEF is intuitive, the comparison between ABC and the low-risk group is less straightforward. Why did DEF and low-risk

adolescents exhibit similar patterns of neuroplasticity when the latter did not experience parenting-related early adversity?

In a recent review by Tooley et al. (2021), differences in socioemotional status (SES) also showed differential patterns of neuroplasticity, consistent with the stress acceleration hypothesis. Specifically, low SES, even without maltreatment history, may be linked to faster brain development than high SES (see Figure 13). Therefore, the global white matter similarities between the DEF and low-risk groups might reflect shared SES-related effects on brain development. That said, this similarity does not mean these groups are neurodevelopmentally identical. It is possible that at the global level, SES influences the broad maturation patterns, but parenting-specific adversity likely impacts particular brain systems, especially those linked to emotion regulation, executive function, and social processing (McLaughlin & Lambert, 2017). These local differences may not appear in broader measures, such as average FA and MD and global network characteristics. In this context, ABC could have helped to maintain circuit integrity or fostered flexibility in systems most at risk due to early adversity. It is important to underscore that this interpretation remains speculative, given that the present study was not set up to directly test these circuit-level differences. Yet, this interpretation represents significant next steps for future research focused on how parenting challenges affect biological development.

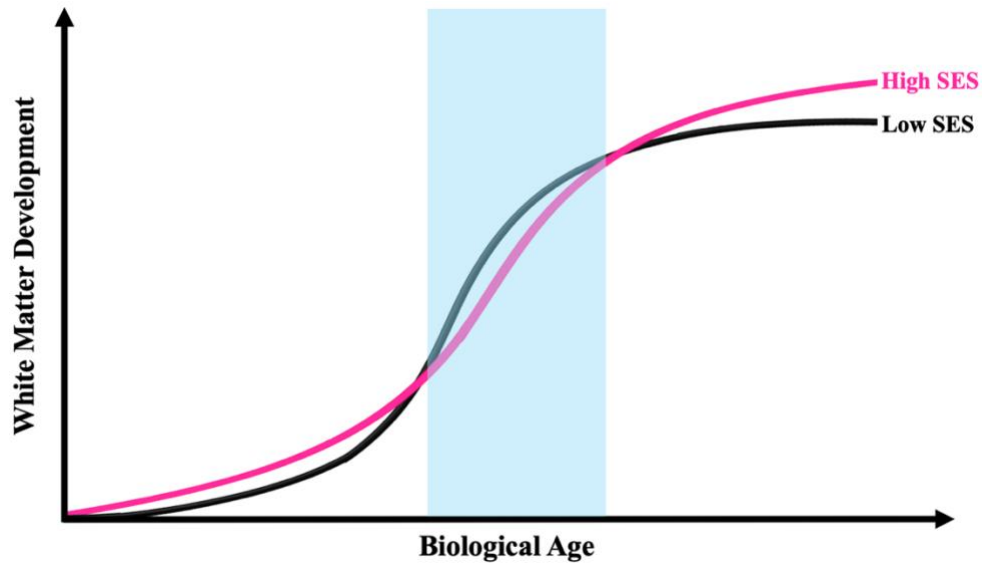


Figure 13. Conceptual Depiction of Associations between SES and White Matter Development (Adapted from Tooley et al., 2021). The black line represents low SES, and the magenta line represents high SES. This figure shows that at the global level, low SES children showed time-limited accelerated maturation of white matter development from middle childhood to adolescence (blue-shaded area).

While these speculations are helpful for generating hypotheses, it is important to ground our interpretations in our data. The fact that ABC youth followed a different developmental trajectory from those of DEF and low-risk aligns with the experiential canalization theory (Blair & Raver, 2012), which proposes that high-quality parenting can redirect developmental pathways even after early adversity. In this context, ABC caregivers are not only viewed as “intervention parents” but also “super parents.” These ABC parents undertook the challenging task of learning and implementing sensitive and nurturing parenting practices while facing economic hardship and involvement in child welfare. Their efforts likely helped create a home environment

that fostered trust and support, which in turn, supported regulatory flexibility as children transitioned into adolescence.

Findings from recent studies within the same sample provide converging evidence for this interpretation (Miller et al., 2024; Valadez et al., 2020; Valadez et al., 2024). Around age 10, children underwent two functional MRI scans: viewing their mother versus a stranger (Valadez et al., 2020) and viewing fearful versus neutral faces (Valadez et al., 2024). ABC children exhibited greater BOLD signal contrast when viewing their mother compared to a stranger, whereas DEF children showed the opposite pattern. Low-risk children fell in between. This BOLD contrast was negatively correlated with parent-reported child behavioral problems and fully mediated the intervention's effects on child behavioral problems. It was also positively correlated with a measure of attachment security, suggesting that neural responses specific to their parents were linked to the quality of the parent-child relationship.

In the emotional face processing task (Valadez et al., 2024), ABC children showed negative amygdala–prefrontal cortex connectivity, a pattern consistent with top-down regulation of emotion. In contrast, DEF children exhibited positive connectivity, while low-risk children again fell between the two intervention groups, showing a negative connectivity pattern similar to ABC. These findings suggest that ABC children, despite early adversity, may have developed emotion regulation circuitry resembling that of low-risk peers. Taken together, these functional MRI findings suggest that early sensitive and nurturing parenting may support neurobiological development. The confluence of different environmental factors (e.g., quality of parenting and SES) may shape the neurodevelopmental pathways.

Further evidence of long-lasting relational effects was seen in adolescence. At age 14, ABC adolescents reported significantly closer relationships with their mothers than DEF adolescents, as indicated by higher scores on the emotional support, companionship, approval, and closeness subscales of the Network Relationship Inventory (Miller et al., 2024). There were no significant differences between ABC and low-risk adolescents, suggesting that early parenting intervention can promote long-lasting secure, trusting parent-child relationships even in the context of adversity. These relational strengths may help explain the more flexible neurodevelopmental trajectory observed in the ABC group.

Early parenting may have laid the groundwork for adaptive reorganization, allowing ABC adolescents to remain open to developmental change and better equipped to meet the increasing emotional, social, and cognitive demands of adolescence. In contrast, DEF adolescents who lacked the benefit of early sensitive parenting may have had to rely on prematurely stabilized neural pathways to meet these demands. However, given the scope of the present study, the link between brain and behavior remains speculative. Future research should investigate whether the extended neuroplasticity observed in the ABC group provides functional advantages in meeting regulatory demands. With this in mind, we offered a few directions informed by our exploratory analyses on individual white matter fasciculi and their functional relevance.

#### **4.4 Exploratory Analyses on Individual White Matter Fasciculi**

As an exploratory effort, we examined intervention effects at the level of specific white matter fasciculi across 43 tracts. Several fasciculi showed significant group differences, even after FDR correction. In the DEF versus ABC contrast,

significant quadratic age interactions emerged in the right anterior thalamic radiation, right dorsal cingulum, and forceps minor. In the low-risk versus ABC contrast, effects extended to the right anterior thalamic radiation, right perigenual cingulum, forceps minor, and the right middle longitudinal fasciculus.

Although exploratory, these patterns suggest that ABC may have preserved or enhanced plasticity in brain systems involved in regulatory and integrative functions. The anterior thalamic radiation, dorsal and perigenual cingulum, and forceps minor have been broadly implicated in executive function, emotion regulation, and social cognition (Bubb et al., 2018; Dufford & Kim, 2017; Norbom et al., 2022). Group differences in these tracts may reflect the impact of early parenting on the maturation of circuits that support affective flexibility and self-regulation. Additionally, the middle longitudinal fasciculus, emerging from the low-risk versus ABC contrast, supports language, reading, and communication capacities (Makris et al., 2013; Park et al., 2023). The flatter trajectory observed in low-risk adolescents could reflect earlier consolidation in these systems, possibly shaped by a relatively stable environmental input compared to ABC. However, a protracted development in these regions, as shown among ABC adolescents, may also be advantageous in the context of sensitive and nurturing parenting and exposure to early adversity. The extended plasticity may support adaptive recalibration following early adversity, potentially reflecting equifinality of developmental pathways, where the routes that individuals take may vary, but they reach similar behavioral endpoints. Together, these fasciculus-level results tentatively suggest that while global white matter patterns may appear similar between DEF and low-risk groups, local circuit-level development may follow distinct

trajectories shaped by both environmentally driven adversity and early parenting quality.

#### **4.5 Strengths and Limitations**

The present study has several noteworthy strengths. First, it leveraged a longitudinal follow-up of an RCT, enabling the testing of causal effects of early parenting interventions on adolescent brain development. Additionally, the use of continuous age improved sensitivity to developmental changes over artificial discrete time points. Employing a mixed-effects modeling approach also offered flexibility in incorporating random effects. To enhance the validity of our interpretations, we included MD alongside FA to better understand the white matter maturation process, rather than relying solely on one DTI metric, which could inevitably lead to misleading interpretations. The inclusion of global network characteristics complemented the interpretations of our findings. Furthermore, our interpretations were based on well-established, theory-driven frameworks (e.g., stress acceleration hypotheses, experiential canalization theory), which shed light on the potential mechanisms underlying the observed group-based differences. Finally, the incorporation of exploratory analyses provided insights for future hypothesis testing to further understand the behavioral correlates of differences in global white matter developmental trajectories.

The study also has some limitations. While grounded in theory, some interpretations (e.g., adaptive recalibration, equifinality) are speculative and extend beyond the direct evidence provided by the current data. Further research is necessary to increase our confidence in these assumptions. A reasonable next step to accomplish this is to test the behavioral correlates directly. A mediation framework could enhance

our understanding of how extended neuroplasticity emerged and the developmental benefits (e.g., emotion regulation, executive functioning) that flexible white matter development affords. In addition, given that the effects of accelerated global white matter maturation could be partially explained by shared socioeconomic risk across DEF and low-risk groups, the next step could involve evaluating the effects of the income-to-needs ratio, neighborhood risks, and community-level child opportunities for support and resources to disentangle the observed effects on white matter development. From an analytic standpoint, the present study focused on the white matter development at the global level. Given that different exposures to early adversity may affect subnetworks or circuits uniquely, our current analytic approach is not equipped to address these nuances. The exploratory analyses, while informative, remain speculative. Ideally, future studies would preregister these analyses prior to replication. Nonetheless, they provide promising targets for mechanistic hypotheses about how early parenting interventions may scaffold the development of brain systems that support adaptive functioning. Finally, during the model development phase, fitting random slopes of linear and quadratic time both produced singularity errors, and showed a suboptimal fit compared to the random intercept model. While these data-driven approaches are well-supported by the literature, the current modeling approach assumes no statistically meaningful variability in how individuals within each group change across time. Modeling growth changes as fixed effects may be an atypical assumption in the context of biological changes, where the rate of biological changes likely varies between individuals in the same group.

Together, these strengths underscore the value of integrating longitudinal, theory-informed, and methodologically rigorous approaches in examining how early

parenting shapes neurodevelopment. Despite these limitations, the findings provide a compelling foundation for future studies aimed at elucidating the mechanisms through which early intervention may promote long-term neurobiological flexibility. Ultimately, this work contributes to a growing body of literature suggesting that sensitive parenting in infancy can have a lasting impact on the adolescent brain, potentially altering developmental trajectories in ways that support resilience and adaptive functioning.

#### **4.6 Conclusion**

The present study provides longitudinal evidence that promoting early sensitive and nurturing parenting, despite a prior history of risk, can optimize the trajectory of adolescent white matter development. We identified distinct developmental patterns among adolescents whose parents received the ABC intervention in infancy, compared to a control intervention and no maltreatment history comparison. Findings highlight the potential for early sensitive and nurturing parenting to promote neuroplasticity and support adaptive recalibration. While further research is essential to understand the behavioral correlates of these neural findings, the present findings support the idea that the quality of early parenting practices has a long-lasting impact on neurodevelopmental flexibility and underscore the importance of early intervention efforts for children exposed to parenting-related adversity.

## REFERENCES

- Andersson, J. L. R., & Sotiropoulos, S. N. (2016). An integrated approach to correction for off-resonance effects and subject movement in diffusion MR imaging. *NeuroImage*, *125*, 1063–1078.
- Andersson, J. L., Skare, S., & Ashburner, J. (2003). How to correct susceptibility distortions in spin-echo echo-planar images: application to diffusion tensor imaging. *NeuroImage*, *20*(2), 870–888.
- Ainsworth, M. D. S., Bell, S. M., & Stayton, D. F. (1974). Infant-mother attachment and social development: Socialization as a product of reciprocal responsiveness to signals. In M. P. M. Richards (Ed.), *The integration of a child into a social world*. (pp. 99–135). Cambridge University Press.
- Baker, A. E., Galván, A., & Fuligni, A. J. (2025). The connecting brain in context: How adolescent plasticity supports learning and development. *Developmental Cognitive Neuroscience*, *71*, 101486.
- Bates, D., Mächler, M., Bolker, B., & Walker, S. (2015). Fitting linear mixed-effects models using lme4. *Journal of Statistical Software*, *67*(1), 1–48.
- Berens, A. E., & Nelson, C. A. (2019). Neurobiology of fetal and infant development. In Zeanah, C. H. (Ed.), *Handbook of infant mental health*. (pp. 41-62). The Guilford Press.
- Bernard, K., Butzin-Dozier, Z., Rittenhouse, J., & Dozier, M. (2010). Cortisol production patterns in young children living with birth parents vs children placed in foster care following involvement of Child Protective Services. *Archives of Pediatrics & Adolescent Medicine*, *164*(5), 438–443. <https://doi.org/10.1001/archpediatrics.2010.54>
- Bernard, K., Dozier, M., Bick, J., Lewis-Morrarty, E., Lindhiem, O., & Carlson, E. (2012). Enhancing attachment organization among maltreated children: results of a randomized clinical trial. *Child Development*, *83*(2), 623–636.
- Bernard, K., Dozier, M., Bick, J., & Gordon, M. K. (2015). Intervening to enhance cortisol regulation among children at risk for neglect: Results of a randomized clinical trial. *Development and Psychopathology*, *27*(3), 829-841.

- Bernard, K., Hostinar, C. E., & Dozier, M. (2015). Intervention effects on diurnal cortisol rhythms of Child Protective Services–referred infants in early childhood: Preschool follow-up results of a randomized clinical trial. *JAMA Pediatrics*, *169*(2), 112-119.
- Bernard, K., Lee, A. H., & Dozier, M. (2017). Effects of the ABC Intervention on foster children’s receptive vocabulary: Follow-up results from a randomized clinical trial. *Child Maltreatment*, *22*(2), 174–179.  
<https://doi.org/10.1177/1077559517691126>
- Bethlehem, R. A. I., Seidlitz, J., White, S. R., Vogel, J. W., Anderson, K. M., Adamson, C., Adler, S., Alexopoulos, G. S., Anagnostou, E., Areces-Gonzalez, A., Astle, D. E., Auyeung, B., Ayub, M., Bae, J., Ball, G., Baron-Cohen, S., Beare, R., Bedford, S. A., Benegal, V., Beyer, F., ... Alexander-Bloch, A. F. (2022). Brain charts for the human lifespan. *Nature*, *604*(7906), 525–533.
- Bick, J., & Dozier, M. (2013). The effectiveness of an attachment-based intervention in promoting foster mothers’ sensitivity toward foster infants. *Infant Mental Health Journal*, *34*(2), 95-103.
- Bick, J., & Nelson, C. A. (2016). Early adverse experiences and the developing brain. *Neuropsychopharmacology*, *41*(1), 177–196.  
<https://doi.org/10.1038/npp.2015.252>
- Bick, J., Palmwood, E. N., Zajac, L., Simons, R., & Dozier, M. (2019). Early Parenting Intervention and Adverse Family Environments Affect Neural Function in Middle Childhood. *Biological Psychiatry*, *85*(4), 326–335.  
<https://doi.org/10.1016/j.biopsych.2018.09.020>
- Bick, J., Zeanah, C. H., Fox, N. A., & Nelson, C. A. (2018). Memory and executive functioning in 12-year-old children with a history of institutional rearing. *Child Development*, *89*(2), 495–508. <https://doi.org/10.1111/cdev.12952>
- Blair, C., & Raver, C. C. (2012). Child development in the context of adversity: Experiential canalization of brain and behavior. *American Psychologist*, *67*(4), 309–318. <https://doi.org/10.1037/a0027493>
- Bowlby, J. (1977). The making and breaking of affectional bonds: I. Aetiology and psychopathology in the light of attachment theory. *The British Journal of Psychiatry*, *130*, 201–210. <https://doi.org/10.1192/bjp.130.3.201>

- Bubb, E. J., Metzler-Baddeley, C., & Aggleton, J. P. (2018). The cingulum bundle: Anatomy, function, and dysfunction. *Neuroscience & Biobehavioral Reviews*, *92*, 104–127.
- Bullmore, E., & Sporns, O. (2009). Complex brain networks: graph theoretical analysis of structural and functional systems. *Nature Reviews Neuroscience*, *10*(3), 186–198. <https://doi.org/10.1038/nrn2575>
- Caballero, A., & Tseng, K. Y. (2016). GABAergic function as a limiting factor for prefrontal maturation during adolescence. *Trends in Neurosciences*, *39*(7), 441–448.
- Callaghan, B. L., & Tottenham, N. (2016). The stress acceleration hypothesis: Effects of early-life adversity on emotion circuits and behavior. *Current Opinion in Behavioral Sciences*, *7*, 76–81. <https://doi.org/10.1016/j.cobeha.2015.11.018>
- Caron, E. B., Bernard, K., & Dozier, M. (2018). In vivo feedback predicts parent behavior change in the attachment and biobehavioral catch-up intervention. *Journal of Clinical Child and Adolescent Psychology*, *47*(sup1), S35–S46. <https://doi.org/10.1080/15374416.2016.1141359>
- Casey, B. J., Cannonier, T., Conley, M. I., Cohen, A. O., Barch, D. M., Heitzeg, M. M., Soules, M. E., Teslovich, T., Dellarco, D. V., & Garavan, H. (2018). The adolescent brain cognitive development (ABCD) study: Imaging acquisition across 21 sites. *Developmental Cognitive Neuroscience*, *32*, 43–54.
- Casey, B. J., Cohen, A. O., & Galván, A. (2025). The beautiful adolescent brain: An evolutionary developmental perspective. *Annals of the New York Academy of Sciences*, *1546*(1), 58–74.
- Ciavarro, M., Grande, E., Bevacqua, G., Morace, R., Ambrosini, E., Pavone, L., ... & Esposito, V. (2022). Structural brain network reorganization following anterior callosotomy for colloid cysts: Connectometry and graph analysis results. *Frontiers in Neurology*, *13*, 894157.
- De Brito, S. A., Viding, E., Sebastian, C. L., Kelly, P. A., Mechelli, A., Maris, H., & McCrory, E. J. (2013). Reduced orbitofrontal and temporal grey matter in a community sample of maltreated children. *Journal of Child Psychology and Psychiatry*, *54*(1), 105–112.
- Dozier, M., & Bernard, K. (2019). *Coaching parents of vulnerable infants: The Attachment and Biobehavioral Catch-up Approach*. Guilford Publications.

- Drury, S. S., Sánchez, M. M., & Gonzalez, A. (2016). When mothering goes awry: Challenges and opportunities for utilizing evidence across rodent, nonhuman primate and human studies to better define the biological consequences of negative early caregiving. *Hormones and Behavior*, *77*, 182–192. <https://doi.org/10.1016/j.yhbeh.2015.10.007>
- Dufford, A. J., & Kim, P. (2017). Family income, cumulative risk exposure, and white matter structure in middle childhood. *Frontiers in Human Neuroscience*, *11*, 547.
- Edmiston, E. E., Wang, F., Mazure, C. M., Guiney, J., Sinha, R., Mayes, L. C., & Blumberg, H. P. (2011). Corticostriatal-limbic gray matter morphology in adolescents with self-reported exposure to childhood maltreatment. *Archives of Pediatrics & Adolescent Medicine*, *165*(12), 1069–1077. <https://doi.org/10.1001/archpediatrics.2011.565>
- Fair, D. A., Cohen, A. L., Power, J. D., Dosenbach, N. U. F., Church, J. A., Miezin, F. M., Schlaggar, B. L., & Petersen, S. E. (2009). Functional brain networks develop from a “local to distributed” organization. *PLoS Computational Biology*, *5*(5), e1000381. <https://doi.org/10.1371/journal.pcbi.1000381>
- Figley, C. R., Uddin, M. N., Wong, K., Kornelsen, J., Puig, J., & Figley, T. D. (2022). Potential Pitfalls of Using Fractional Anisotropy, Axial Diffusivity, and Radial Diffusivity as Biomarkers of Cerebral White Matter Microstructure. *Frontiers in Neuroscience*, *15*. <https://doi.org/10.3389/fnins.2021.799576>
- Fox, N. A., & Rutter, M. (2010). Introduction to the special section on the effects of early experience on development. *Child Development*, *81*(1), 23-27.
- Fuster J. M. (2001). The prefrontal cortex -- an update: Time is of the essence. *Neuron*, *30*(2), 319–333. [https://doi.org/10.1016/s0896-6273\(01\)00285-9](https://doi.org/10.1016/s0896-6273(01)00285-9)
- Gao, W., Zhu, H., Giovanello, K. S., Smith, J. K., Shen, D., Gilmore, J. H., & Lin, W. (2009). Evidence on the emergence of the brain's default network from 2-week-old to 2-year-old healthy pediatric subjects. *Proceedings of the National Academy of Sciences of the United States of America*, *106*(16), 6790–6795. <https://doi.org/10.1073/pnas.0811221106>
- Garnett, M., Bernard, K., Hoyer, J., Zajac, L., & Dozier, M. (2020). Parental sensitivity mediates the sustained effect of Attachment and Biobehavioral Catch-up on cortisol in middle childhood: A randomized clinical trial. *Psychoneuroendocrinology*, *121*, 104809. <https://doi.org/10.1016/j.psyneuen.2020.104809>

- Gee, D. G., Gabard-Durnam, L. J., Flannery, J., Goff, B., Humphreys, K. L., Telzer, E. H., Hare, T. A., Bookheimer, S. Y., & Tottenham, N. (2013). Early developmental emergence of human amygdala-prefrontal connectivity after maternal deprivation. *Proceedings of the National Academy of Sciences of the United States of America*, *110*(39), 15638–15643. <https://doi.org/10.1073/pnas.1307893110>
- Giedd, J. N., Blumenthal, J., Jeffries, N. O., Castellanos, F. X., Liu, H., Zijdenbos, A., Paus, T., Evans, A. C., & Rapoport, J. L. (1999). Brain development during childhood and adolescence: a longitudinal MRI study. *Nature Neuroscience*, *2*(10), 861–863.
- Govindan, R. M., Behen, M. E., Helder, E., Makki, M. I., & Chugani, H. T. (2010). Altered water diffusivity in cortical association tracts in children with early deprivation identified with Tract-Based Spatial Statistics (TBSS). *Cerebral Cortex*, *20*(3), 561–569. <https://doi.org/10.1093/cercor/bhp122>
- Hofer, M. A. (2006). Psychobiological roots of early attachment. *Current Directions in Psychological Science*, *15*(2), 84–88. <https://doi.org/10.1111/j.0963-7214.2006.00412.x>
- Hoye, J. R., Cheishvili, D., Yarger, H. A., Roth, T. L., Szyf, M., & Dozier, M. (2020). Preliminary indications that the Attachment and Biobehavioral Catch-up Intervention alters DNA methylation in maltreated children. *Development and Psychopathology*, *32*(4), 1486–1494. <https://doi.org/10.1017/S0954579419001421>
- Huang, H., Gundapuneedi, T., & Rao, U. (2012). White matter disruptions in adolescents exposed to childhood maltreatment and vulnerability to psychopathology. *Neuropsychopharmacology*, *37*(12), 2693–2701. <https://doi.org/10.1038/npp.2012.133>
- Jackowski, A. P., Douglas-Palumberi, H., Jackowski, M., Win, L., Schultz, R. T., Staib, L. W., ... & Kaufman, J. (2008). Corpus callosum in maltreated children with posttraumatic stress disorder: a diffusion tensor imaging study. *Psychiatry Research: Neuroimaging*, *162*(3), 256–261.
- Jaffee S. R. (2017). Child maltreatment and risk for psychopathology in childhood and adulthood. *Annual Review of Clinical Psychology*, *13*, 525–551. <https://doi.org/10.1146/annurev-clinpsy-032816-045005>

- Jedd, K., Hunt, R. H., Cicchetti, D., Hunt, E., Cowell, R. A., Rogosch, F. A., Toth, S. L., & Thomas, K. M. (2015). Long-term consequences of childhood maltreatment: Altered amygdala functional connectivity. *Development and Psychopathology*, *27*(4 Pt 2), 1577–1589.  
<https://doi.org/10.1017/S0954579415000954>
- Kelly, P. A., Viding, E., Wallace, G. L., Schaer, M., De Brito, S. A., Robustelli, B., & McCrory, E. J. (2013). Cortical thickness, surface area, and gyrification abnormalities in children exposed to maltreatment: Neural markers of vulnerability? *Biological Psychiatry*, *74*(11), 845-852.
- Kennedy, B. V., Hanson, J. L., Buser, N. J., van den Bos, W., Rudolph, K. D., Davidson, R. J., & Pollak, S. D. (2021). Accumbens tract integrity is related to early life adversity and feedback learning. *Neuropsychopharmacology*, *46*(13), 2288-2294.
- Kim, D. J., & Min, B. K. (2020). Rich-club in the brain's macrostructure: Insights from graph theoretical analysis. *Computational and Structural Biotechnology Journal*, *18*, 1761-1773.
- Kolb, B., & Gibb, R. (2011). Brain plasticity and behaviour in the developing brain. *Journal of the Canadian Academy of Child and Adolescent Psychiatry*, *20*(4), 265–276.
- Korom, M., Goldstein, A., Tabachnick, A. R., Palmwood, E. N., Simons, R. F., & Dozier, M. (2021). Early parenting intervention accelerates inhibitory control development among CPS-involved children in middle childhood: A randomized clinical trial. *Developmental Science*, *24*(3), e13054.  
<https://doi.org/10.1111/desc.13054>
- Kuznetsova, A., Brockhoff, P. B., & Christensen, R. H. B. (2017). lmerTest package: Tests in linear mixed effects models. *Journal of Statistical Software*, *82*(13), 1–26. <https://doi.org/10.18637/jss.v082.i13>
- Lebel, C., & Beaulieu, C. (2011). Longitudinal development of human brain wiring continues from childhood into adulthood. *Journal of Neuroscience*, *31*(30), 10937–10947. <https://doi.org/10.1523/JNEUROSCI.5302-10.2011>
- Lebel, C., Gee, M., Camicioli, R., Wieler, M., Martin, W., & Beaulieu, C. (2012). Diffusion tensor imaging of white matter tract evolution over the lifespan. *NeuroImage*, *60*(1), 340–352.  
<https://doi.org/10.1016/j.neuroimage.2011.11.094>

- Lebel, C., Treit, S., & Beaulieu, C. (2017). A review of diffusion MRI of typical white matter development from early childhood to young adulthood. *NMR in Biomedicine*, *32*(1), e3778.
- Lee, D. A., Lee, H. J., & Park, K. M. (2023). Structural brain network analysis in occipital lobe epilepsy. *BMC neurology*, *23*(1), 268.
- Letarte, M. J., Normandeau, S., & Allard, J. (2010). Effectiveness of a parent training program "Incredible Years" in a child protection service. *Child Abuse & Neglect*, *34*(4), 253–261.
- Lind, T., Bernard, K., Ross, E., & Dozier, M. (2014). Intervention effects on negative affect of CPS-referred children: Results of a randomized clinical trial. *Child Abuse & Neglect*, *38*(9), 1459-1467.
- Lind, T., Bernard, K., Yarger, H. A., & Dozier, M. (2020). Promoting compliance in children referred to child protective services: A randomized clinical trial. *Child Development*, *91*(2), 563-576.
- Makris, N., Kennedy, D. N., McInerney, S., Sorensen, A. G., Wang, R., Caviness, V. S., & Pandya, D. N. (2013). Human middle longitudinal fascicle: Segregation and overlap with the arcuate fascicle revealed by diffusion tensor imaging. *Brain Structure and Function*, *218*(4), 951–968.
- McCarthy-Jones, S., Oestreich, L. K. L., Lyall, A. E., Kikinis, Z., Newell, D. T., Savadjiev, P., Shenton, M. E., Kubicki, M., Pasternak, O., Whitford, T. J., & Australian Schizophrenia Research Bank (2018). Childhood adversity associated with white matter alteration in the corpus callosum, corona radiata, and uncinate fasciculus of psychiatrically healthy adults. *Brain Imaging and Behavior*, *12*(2), 449–458. <https://doi.org/10.1007/s11682-017-9703-1>
- McCrary, E., De Brito, S. A., & Viding, E. (2011). The impact of childhood maltreatment: a review of neurobiological and genetic factors. *Frontiers in Psychiatry*, *2*, 48. <https://doi.org/10.3389/fpsyt.2011.00048>
- McLaughlin, K. A., & Lambert, H. K. (2017). Child trauma exposure and psychopathology: Mechanisms of risk and resilience. *Current Opinion in Psychology*, *14*, 29–34.
- Miller, K. N., Bourne, S. V., Dahl, C. M., Costello, C., Attinelly, J., Jennings, K., & Dozier, M. (2024). Using randomized controlled trials to ask questions regarding developmental psychopathology: A tribute to Dante Cicchetti. *Development and Psychopathology*, *36*(5), 2305-2314.

- Miller, D. J., Duka, T., Stimpson, C. D., Schapiro, S. J., Baze, W. B., McArthur, M. J., Fobbs, A. J., Sousa, A. M. M., Sestan, N., Wildman, D. E., Lipovich, L., Kuzawa, C. W., Hof, P. R., & Sherwood, C. C. (2012). Prolonged myelination in human neocortical evolution. *Proceedings of the National Academy of Sciences of the United States of America*, *109*(41), 16480-16485.
- Mills, K. L., Goddings, A.-L., Clasen, L. S., Giedd, J. N., & Blakemore, S.-J. (2016). Structural brain development between childhood and adulthood: Convergence across four longitudinal samples. *NeuroImage*, *141*, 273–281. <https://doi.org/10.1016/j.neuroimage.2016.07.044>
- Moini, J., & Piran, P. (2020). *Functional and clinical Neuroanatomy: A guide for health care professionals*. Academic Press.
- Nelson, C. A. III, Zeanah, C. H., & Fox, N. A. (2019). How early experience shapes human development: The case of psychosocial deprivation. *Neural Plasticity*, *2019*, Article 1676285. <https://doi.org/10.1155/2019/1676285>
- Norbom, L. B., Alnæs, D., Kaufmann, T., Andreassen, O. A., Westlye, L. T., & Tamnes, C. K. (2022). Probing brain developmental patterns of myelination and associations with psychopathology in youth using gray/white matter contrast. *Neuroscience & Biobehavioral Reviews*, *132*, 1057–1072.
- Ochsner, K. N., & Gross, J. J. (2005). The cognitive control of emotion. *Trends in Cognitive Sciences*, *9*(5), 242–249. <https://doi.org/10.1016/j.tics.2005.03.010>
- Ohashi, K., Anderson, C. M., Bolger, E. A., Khan, A., McGreenery, C. E., & Teicher, M. H. (2017). Childhood maltreatment is associated with alteration in global network fiber-tract architecture independent of history of depression and anxiety. *NeuroImage*, *150*, 50-59.
- Park, J., Smith, A. B., & Lee, C. (2023). A narrative review of the middle longitudinal fasciculus: Anatomy, function, and clinical relevance. *Frontiers in Human Neuroscience*, *17*, Article 1139292.
- Phelps, E. A. (2004). Human emotion and memory: interactions of the amygdala and hippocampal complex. *Current Opinion in Neurobiology*, *14*(2), 198-202.
- Puetz, V. B., Viding, E., Palmer, A., Kelly, P. A., Lickley, R., Koutoufa, I., Sebastian, C. L., & McCrory, E. J. (2016). Altered neural response to rejection-related words in children exposed to maltreatment. *Journal of Child Psychology and Psychiatry*, *57*(10), 1165–1173. <https://doi.org/10.1111/jcpp.12595>

- R Core Team. (2023). R: A language and environment for statistical computing. *R Foundation for Statistical Computing*. <https://www.R-project.org/>
- Raby, K. L., Freedman, E., Yarger, H. A., Lind, T., & Dozier, M. (2019). Enhancing the language development of toddlers in foster care by promoting foster parents' sensitivity: Results from a randomized controlled trial. *Developmental Science*, 22(2), e12753.
- Ramey, C. T., Yeates, K. O., & Short, E. J. (1984). The plasticity of intellectual development: Insights from preventive intervention. *Child Development*, 55(5), 1913–1925.
- Rowe, M., Siow, B., Alexander, D. C., Ferizi, U., & Richardson, S. (2016). Concepts of diffusion in MRI. In Hecke, W. V., Emsell, L., & Sunaert, S. (Eds.), *Diffusion tensor imaging: A practical handbook*. (pp. 23-35). Springer.
- Sampaio-Baptista, C., & Johansen-Berg, H. (2017). White matter plasticity in the adult brain. *Neuron*, 96(6), 1239–1251.
- Schumacher, M., Ghomari, A., Mattern, C., Bougnères, P., & Traiffort, E. (2021). Testosterone and myelin regeneration in the central nervous system. *Androgens: Clinical Research and Therapeutics*, 2(1), 231-251.
- Serra, M., De Pisapia, N., Rigo, P., Papinutto, N., Jager, J., Bornstein, M. H., & Venuti, P. (2016). Secure attachment status is associated with white matter integrity in healthy young adults. *NeuroReport*, 26(18), 1106.
- Sheldrick, R. C., Schlichting, L. E., Berger, B., Clyne, A., Ni, P., Perrin, E. C., & Vivier, P. M. (2019). Establishing new norms for developmental milestones. *Pediatrics*, 144(6), e20190374. <https://doi.org/10.1542/peds.2019-0374>
- Simmonds, D. J., Hallquist, M. N., Asato, M., & Luna, B. (2014). Developmental stages and sex differences of white matter and behavioral development through adolescence: A longitudinal diffusion tensor imaging (DTI) study. *NeuroImage*, 92, 356–368. <https://doi.org/10.1016/j.neuroimage.2013.12.044>
- Smith, S. M., Jenkinson, M., Woolrich, M. W., Beckmann, C. F., Behrens, T. E., Johansen-Berg, H., Bannister, P. R., De Luca, M., Drobnjak, I., Flitney, D. E., Niazy, R. K., Saunders, J., Vickers, J., Zhang, Y., De Stefano, N., Brady, J. M., & Matthews, P. M. (2004). Advances in functional and structural MR image analysis and implementation as FSL. *NeuroImage*, 23 Suppl 1, S208–S219. <https://doi.org/10.1016/j.neuroimage.2004.07.051>

- Smith, S. M., Jenkinson, M., Johansen-Berg, H., Rueckert, D., Nichols, T. E., Mackay, C. E., Watkins, K. E., Ciccarelli, O., Cader, M. Z., Matthews, P. M., & Behrens, T. E. (2006). Tract-based spatial statistics: Voxelwise analysis of multi-subject diffusion data. *NeuroImage*, *31*(4), 1487–1505. <https://doi.org/10.1016/j.neuroimage.2006.02.024>
- Steenhoff, T., Tharner, A., & Væver, M. S. (2019). Mothers' and fathers' observed interaction with preschoolers: Similarities and differences in parenting behavior in a well-resourced sample. *PLoS ONE*, *14*(8), 25. <https://doi.org/10.1371/journal.pone.0221661>
- Swenson, C. C., Schaeffer, C. M., Henggeler, S. W., Faldowski, R., & Mayhew, A. M. (2010). Multisystemic therapy for child abuse and neglect: A randomized effectiveness trial. *Journal of Family Psychology*, *24*(4), 497–507. <https://doi.org/10.1037/a0020324>
- Tabachnick, A. R., Raby, K. L., Goldstein, A., Zajac, L., & Dozier, M. (2019). Effects of an attachment-based intervention in infancy on children's autonomic regulation during middle childhood. *Biological Psychology*, *143*, 22–31. <https://doi.org/10.1016/j.biopsycho.2019.01.006>
- Tamnes, C. K., Overbye, K., Ferschmann, L., Fjell, A. M., Walhovd, K. B., Blakemore, S. J., & Dumontheil, I. (2018). Social perspective taking is associated with self-reported prosocial behavior and regional cortical thickness across adolescence. *Developmental Psychology*, *54*(9), 1745–1757. <https://doi.org/10.1037/dev0000541>
- Tau, G. Z., & Peterson, B. S. (2010). Normal development of brain circuits. *Neuropsychopharmacology*, *35*(1), 147–168. <https://doi.org/10.1038/npp.2009.115>
- Teicher, M. H., Samson, J. A., Anderson, C. M., & Ohashi, K. (2016). The effects of childhood maltreatment on brain structure, function and connectivity. *Nature Reviews Neuroscience*, *17*(10), 652–666. <https://doi.org/10.1038/nrn.2016.111>
- Tooley, U. A., Bassett, D. S., & Mackey, A. P. (2021). Environmental influences on the pace of brain development. *Nature Reviews Neuroscience*, *22*(6), 372–384. <https://doi.org/10.1038/s41583-021-00457-5>
- Tottenham N. (2012). Risk and developmental heterogeneity in previously institutionalized children. *The Journal of Adolescent Health*, *51*(2 Suppl), S29–S33. <https://doi.org/10.1016/j.jadohealth.2012.04.004>

- Tottenham, N. (2013). The importance of early experiences for neuro-affective development. In Andersen, S., & Pine, D. (Eds.), *The neurobiology of childhood: Current topics in behavioral neurosciences, Vol 16*. (pp. 109-129). Springer.
- Tottenham N. (2020). Early adversity and the neotenus human brain. *Biological Psychiatry*, 87(4), 350–358. <https://doi.org/10.1016/j.biopsych.2019.06.018>
- Tozzi, L., Garczarek, L., Janowitz, D., Stein, D. J., Wittfeld, K., Dobrowolny, H., Lagopoulos, J., Hatton, S. N., Hickie, I. B., & Carballo, A. (2020). Interactive impact of childhood maltreatment, depression, and age on cortical brain structure: Mega-analytic findings from a large multi-site cohort. *Psychological Medicine*, 50(6), 1020–1031.
- Tronick, E. (2007). *The neurobehavioral and social-emotional development of infants and children*. Norton & Co.
- Valadez, E. A., Tottenham, N., Korom, M., Tabachnick, A. R., Pine, D. S., & Dozier, M. (2024). A randomized controlled trial of a parenting intervention during infancy alters amygdala-prefrontal circuitry in middle childhood. *Journal of the American Academy of Child and Adolescent Psychiatry*, S0890-8567(23)00343-X. Advance online publication. <https://doi.org/10.1016/j.jaac.2023.06.015>
- Valadez, E. A., Tottenham, N., Tabachnick, A. R., & Dozier, M. (2020). Early parenting intervention effects on brain responses to maternal cues among high-risk children. *The American Journal of Psychiatry*, 177(9), 818–826. <https://doi.org/10.1176/appi.ajp.2020.20010011>
- van der Voort, A., Linting, M., Juffer, F., Schoenmaker, C., Bakermans-Kranenburg, M., & van IJzendoorn, M. H. (2014). More than two decades after adoption: Associations between infant attachment, early maternal sensitivity and the diurnal cortisol curve of adopted young adults. *Children and Youth Services Review*, 46, 186-194. <https://doi.org/10.1016/j.chidyouth.2014.08.022>
- van Essen, D. C., Ugurbil, K., Auerbach, E., Barch, D., Behrens, T. E. J., Bucholz, R., Chang, A., Chen, L., Corbetta, M., Curtiss, S. W., Della Penna, S., Feinberg, D., Glasser, M. F., Harel, N., Heath, A. C., Larson-Prior, L., Marcus, D., Michalareas, G., Moeller, S., ... Yacoub, E. (2012). The human connectome project: A data acquisition perspective. *NeuroImage*, 62(4), 2222–2231. <https://doi.org/10.1016/j.neuroimage.2012.02.018>

- Warrington, S., Bryant, K. L., Khrapitchev, A. A., Sallet, J., Charquero-Ballester, M., Douaud, G., ... & Sotiropoulos, S. N. (2020). XTRACT-Standardised protocols for automated tractography in the human and macaque brain. *Neuroimage*, *217*, 116923. <https://doi.org/10.1016/j.neuroimage.2020.116923>
- Whitaker, K. J., Vértes, P. E., Romero-Garcia, R., Váša, F., Moutoussis, M., Prabhu, G., Weiskopf, N., Callaghan, M. F., Wagstyl, K., Rittman, T., Tait, R., Ooi, C., Suckling, J., Inkster, B., Fonagy, P., Dolan, R. J., Jones, P. B., Goodyer, I. M., & Bullmore, E. T. (2016). Adolescence is associated with genomically patterned consolidation of the hubs of the human brain connectome. *Proceedings of the National Academy of Sciences*, *113*(32), 9105–9110. <https://doi.org/10.1073/pnas.1601745113>
- Whittle, S., Simmons, J. G., Dennison, M., Vijayakumar, N., Schwartz, O., Yap, M. B., ... & Allen, N. B. (2014). Positive parenting predicts the development of adolescent brain structure: A longitudinal study. *Developmental Cognitive Neuroscience*, *8*, 7-17.
- Whittle, S., Vijayakumar, N., Dennison, M., Schwartz, O., Simmons, J. G., Sheeber, L., & Allen, N. B. (2016). Observed measures of negative parenting predict brain development during adolescence. *PloS ONE*, *11*(1), e0147774.
- Wickham, H. (2016). *ggplot2: Elegant graphics for data analysis*. Springer-Verlag New York.
- Yarger, H. A., Bernard, K., Caron, E. B., Wallin, A., & Dozier, M. (2020). Enhancing parenting quality for young children adopted internationally: Results of a randomized controlled trial. *Journal of Clinical Child and Adolescent Psychology*, *49*(3), 378–390. <https://doi.org/10.1080/15374416.2018.1547972>
- Yeh, F. C., Verstynen, T. D., Wang, Y., Fernández-Miranda, J. C., & Tseng, W. Y. I. (2013). Deterministic diffusion fiber tracking improved by quantitative anisotropy. *PloS ONE*, *8*(11), e80713.

## Appendix A

### IRB/HUMAN SUBJECTS APPROVAL



Institutional Review Board  
210H HULLIHEN HALL  
NEWARK, DE 19716  
PHONE: 302-831-2137  
FAX: 302-831-2828

DATE: May 9, 2025

TO: Mary Dozier, PhD  
FROM: University of Delaware IRB

STUDY TITLE: [1437202-20] Key Adolescent Outcomes: fMRI Task  
SUBMISSION TYPE: Continuing Review/Progress Report

ACTION: APPROVED - Data Analysis Only  
APPROVAL DATE: May 9, 2025  
EXPIRATION DATE: May 14, 2026  
REVIEW TYPE: Expedited Review  
REVIEW CATEGORY: Expedited review category # 8(c)

Thank you for your Continuing Review/Progress Report submission to the University of Delaware Institutional Review Board (UD IRB). The UD IRB has reviewed and APPROVED the proposed research and submitted documents via Expedited Review in compliance with the pertinent federal regulations.

As the Principal Investigator for this study, you are responsible for and agree that:

- All research must be conducted in accordance with the protocol and all other study forms as approved in this submission. Any revisions to the approved study procedures or documents must be reviewed and approved by the IRB prior to their implementation. Please use the UD amendment form to request the review of any changes to approved study procedures or documents.
- Informed consent is a process that must allow prospective participants sufficient opportunity to discuss and consider whether to participate. IRB-approved and stamped consent documents must be used when enrolling participants and a written copy shall be given to the person signing the informed consent form.
- Unanticipated problems, serious adverse events involving risk to participants, and all non-compliance issues must be reported to this office in a timely fashion according with the UD requirements for reportable events. All sponsor reporting requirements must also be followed.

Oversight of this study by the UD IRB REQUIRES the submission of a CONTINUING REVIEW seeking the renewal of this IRB approval, which will expire on May 14, 2026. A continuing review/progress report form and up-to-date copies of the protocol form and all other approved study materials must be submitted to the UD IRB at least 45 days prior to the expiration date to allow for the required IRB review of that report.

If you have any questions, please contact the UD IRB Office at (302) 831-2137 or via email at [hsrb-research@udel.edu](mailto:hsrb-research@udel.edu). Please include the study title and reference number in all correspondence with this office.